phase with a dilated cardiomyopathy phenotype, by direct injection into the myocardium [7]. In the present study, however, MSC were transplanted 1 week following myosin injection, corresponding to the acute phase of myocarditis, by intravenous injection, because this model is more relevant to clinical situations. Myosin injection caused acute heart failure as indicated by increased LVEDP and decreased Max d*P*/d*t* and %FS, and 2 out of 15 rats died; however, intravenous injection of MSC in the acute phase significantly improved the heart failure as determined by improvement of these parameters, and no death was observed.

Wang et al. have shown that embryonic stem (ES) cells transplanted into a mouse model of myocarditis regenerate cardiomyocytes, decrease inflammation and increase survival, possibly through migration of ES cells and differentiation into cardiomyocytes [14]. In the present study, we examined the therapeutic potential of transplanted MSC, which are more applicable to clinical situations than ES cells, in a rat model of acute myocarditis. Recent studies have demonstrated that autologous or allogeneic MSC strongly suppress T-lymphocyte proliferation [15,16]. These findings raise the possibility that MSC have the ability to attenuate inflammatory responses. Interestingly, the present study demonstrated that transplantation of MSC attenuated the infiltration of CD68-positive inflammatory cells and the expression of MCP-1 in a rat model of acute myocarditis. MCP-1 is a member of the C–C subfamily of chemokines with chemoattractant activity for major inflammatory cells, and is known to play an important role in the induction of experimental acute myocarditis [17,18]. Cardiac-targeted expression of MCP-1 results in monocyte/macrophage infiltration into the heart, and causes interstitial fibrosis and ventricular chamber dilation [19]. In the myosin-induced acute myocarditis model, MCP-1 expression is increased in the heart from days 15–27 post-myosin injection, and serum MCP-1 level is elevated from days 15–24 [18]. In consistent with this report, our model showed an increase in MCP-1 in the heart and serum on day 21 post-myosin injection, and MSC transplantation attenuated the increase in MCP-1 and the infiltration of CD68-positive inflammatory cells. Furthermore, earlier studies have shown that MSC express CCR2, the receptor for MCP-1, and that MCP-1 promotes the migration of MSC that express CCR2 [20,21]. Thus, it is speculated that MSC secrete some anti-inflammatory factors in response to MCP-1; however, the precise mechanisms for the anti-inflammatory effect still remains to be elucidated.

Because MCP-1 plays an important role in this myosin-induced myocarditis model, we examined the direct effect of MCP-1, besides its chemoattractant activity, on adult rat cardiomyocytes. Our *in vitro* experiment demonstrated that MCP-1 stimulation on cardiomyocytes resulted in an increase of cell injury and death, whereas MSC-derived conditioned medium attenuated these effects. It has been reported that CCR2 expression is increased in the failing myocardium, and MCP-1 stimulation on cardiomyocytes induces other inflammatory cytokines such as IL-1β and IL-6, which may reduce cardiomyocyte contractility partly via induction of apoptosis [22–25]. In addition, our previous and present study demonstrated that cultured MSC secreted large amounts of angiogenic and anti-apoptotic factors such as VEGF, HGF, insulin-like growth factor-1 and adrenomedullin [7]. Furthermore, a recent study demonstrated that conditioned medium obtained from MSC culture had cardioprotective effect [26]. Taken together, although various factors might be involved, MSC might have cardioprotective effects in a paracrine manner in response to MCP-1.

In the present study, MSC transplantation increased capillary density in the myocardium. Improvement in myocardial vascular supply has been shown to decrease necrosis and inflammation in viral myocarditis [8,27,28]. We have previously reported increased capillary density associated with improved cardiac function and decreased infarct size following MSC transplantation in a rat model of myocardial infarction [5]. These results suggest that MSC-induced neovascularization may have contributed to the improvement of cardiac function in this rat model of acute myocarditis. However, when PKH26 dye-labeled MSC were intravenously injected in rats with acute myocarditis, only a small fraction of PKH26-labeled cells were positive for troponin T 2 weeks after transplantation (data not shown). Our previous study demonstrated that ~3% of the intravenously administered MSCs were incorporated into the heart 24 h after transplantation in rats with acute myocardial infarction [5]. Although the animal model and the evaluation time were different, our present study showed that only a small number of administered MSC was differentiated into endothelial cells or cardiomyocytes, thus the contribution of the differentiated MSC to the improvement of cardiac function in this model appears to be rather insignificant.

In conclusion, MSC transplantation attenuated myocardial injury and dysfunction in a rat model of acute myocarditis, at least in part through paracrine effects of MSC.

Acknowledgments

This work was funded by a post-doctoral fellowship from the Japan Society for the Promotion of Science, and research grants for Cardiovascular Disease (16C-6, 17C-1 and 18C-1) and Human Genome Tissue Engineering 009 from the Ministry of Health, Labor and Welfare.

References

[1] Levi D, Alejos J. Diagnosis and treatment of pediatric viral myocarditis. Curr Opin Cardiol 2001;16:77–83.
[2] Feldman AM, McNamara D. Myocarditis. N Engl J Med 2000;343:1388–98.
[3] Pittenger MF, Mackay AM, Beck SC, Jaiswal RK, Douglas R, Mosca JD, et al. Multilineage potential of adult human mesenchymal stem cells. Science 1999;284:143–7.
[4] Le Blanc K, Pittenger M. Mesenchymal stem cells: progress toward promise. Cytotherapy 2005;7:36–45.
[5] Nagaya N, Fujii T, Iwase T, Ohgushi H, Itoh T, Uematsu M, et al. Intravenous administration of mesenchymal stem cells improves cardiac function in rats with acute myocardial infarction through angiogenesis and myogenesis. Am J Physiol: Heart Circ Physiol 2004;287:H2670–6.

[6] Miyahara Y, Nagaya N, Kataoka M, Yanagawa B, Tanaka K, Hao H, et al. Monolayered mesenchymal stem cells repair scarred myocardium after myocardial infarction. Nat Med 2006;12:459–65.
[7] Nagaya N, Kangawa K, Itoh T, Iwase T, Murakami S, Miyahara Y, et al. Transplantation of mesenchymal stem cells improves cardiac function in a rat model of dilated cardiomyopathy. Circulation 2005; 112:1128–35.
[8] Kodama M, Matsumoto Y, Fujiwara M, Masani F, Izumi T, Shibata A. A novel experimental model of giant cell myocarditis induced in rats by immunization with cardiac myosin fraction. Clin Immunol Immunopathol 1990;57:250–62.
[9] Tanaka K, Honda M, Takabatake T. Redox regulation of MAPK pathways and cardiac hypertrophy in adult rat cardiac myocyte. J Am Coll Cardiol 2001;37:676–85.
[10] Kodama M, Matsumoto Y, Fujiwara M, Zhang SS, Hanawa H, Itoh E, et al. Characteristics of giant cells and factors related to the formation of giant cells in myocarditis. Circ Res 1991;69:1042–50.
[11] Fairweather D, Kaya Z, Shellam GR, Lawson CM, Rose NR. From infection to autoimmunity. J Autoimmun 2001;16:175–86.
[12] Cunningham MW. T cell mimicry in inflammatory heart disease. Mol Immunol 2004;40:1121–7.
[13] Kodama M, Hanawa H, Saeki M, Hosono H, Inomata T, Suzuki K, et al. Rat dilated cardiomyopathy after autoimmune giant cell myocarditis. Circ Res 1994;75:278–84.
[14] Wang JF, Yang Y, Wang G, Min J, Sullivan MF, Ping P, et al. Embryonic stem cells attenuate viral myocarditis in murine model. Cell Transplant 2002;11:753–8.
[15] Di Nicola M, Carlo-Stella C, Magni M, Milanesi M, Longoni PD, Matteucci P, et al. Human bone marrow stromal cells suppress T-lymphocyte proliferation induced by cellular or nonspecific mitogenic stimuli. Blood 2002;99: 3838–43.
[16] Tse WT, Pendleton JD, Beyer WM, Egalka MC, Guinan EC. Suppression of allogeneic T-cell proliferation by human marrow stromal cells: implications in transplantation. Transplantation 2003;75:389–97.
[17] Rollins BJ. Chemokines. Blood 1997;90:909–28.
[18] Fuse K, Kodama M, Hanawa H, Okura Y, Ito M, Shiono T, et al. Enhanced expression and production of monocyte chemoattractant protein-1 in myocarditis. Clin Exp Immunol 2001;124:346–52.
[19] Kolattukudy PE, Quach T, Bergese S, Breckenridge S, Hensley J, Altschuld R, et al. Myocarditis induced by targeted expression of the MCP-1 gene in murine cardiac muscle. Am J Pathol 1998;152:101–11.
[20] Ji JF, He BP, Dheen ST, Tay SS. Interactions of chemokines and chemokine receptors mediate the migration of mesenchymal stem cells to the impaired site in the brain after hypoglossal nerve injury. Stem Cells 2004;22:415–27.
[21] Wang L, Li Y, Chen J, Gautam SC, Zhang Z, Lu M, et al. Ischemic cerebral tissue and MCP-1 enhance rat bone marrow stromal cell migration in interface culture. Exp Hematol 2002;30:831–6.
[22] Damas JK, Eiken HG, Oie E, Bjerkeli V, Yndestad A, Ueland T, et al. Myocardial expression of CC- and CXC-chemokines and their receptors in human end-stage heart failure. Cardiovasc Res 2000;47:778–87.
[23] Damas JK, Aukrust P, Ueland T, Odegaard A, Eiken HG, Gullestad L, et al. Monocyte chemoattractant protein-1 enhances and interleukin-10 suppresses the production of inflammatory cytokines in adult rat cardiomyocytes. Basic Res Cardiol 2001;96:345–52.
[24] Ing DJ, Zang J, Dzau VJ, Webster KA, Bishopric NH. Modulation of cytokine-induced cardiac myocyte apoptosis by nitric oxide, Bak, and Bcl-x. Circ Res 1999;84:21–33.
[25] Hirota H, Chen J, Betz UA, Rajewsky K, Gu Y, Ross Jr J, et al. Loss of a gp130 cardiac muscle cell survival pathway is a critical event in the onset of heart failure during biomechanical stress. Cell 1999;97: 189–98.
[26] Gnecchi M, He H, Liang OD, Melo LG, Morello F, Mu H, et al. Paracrine action accounts for marked protection of ischemic heart by Akt-modified mesenchymal stem cells. Nat Med 2005;11:367–8.
[27] Lee JK, Zaidi SH, Liu P, Dawood F, Cheah AY, Wen WH, et al. A serine elastase inhibitor reduces inflammation and fibrosis and preserves cardiac function after experimentally-induced murine myocarditis. Nat Med 1998;4:1383–91.
[28] Ono K, Matsumori A, Shioi T, Furukawa Y, Sasayama S. Contribution of endothelin-1 to myocardial injury in a murine model of myocarditis: acute effects of bosentan, an endothelin receptor antagonist. Circulation 1999;100:1823–9.

JOURNAL OF MATERIALS SCIENCE: MATERIALS IN MEDICINE 17 (2006) 33–41

Observation and quantitative analysis of rat bone marrow stromal cells cultured *in vitro* on newly formed transparent β-tricalcium phosphate

NORIKO KOTOBUKI[1], DAISUKE KAWAGOE[2], DAISHIROU NOMURA[3], YOUICHI KATOU[1], KAORI MURAKI[1], HIROTAKA FUJIMORI[3], SEISHI GOTO[3], KOJI IOKU[2], HAJIME OHGUSHI[1,*]

[1]*Research Institute for Cell Engineering (RICE), National Institute of Advanced Industrial Science and Technology (AIST), 3-11-46 Nakouji, Amagasaki, Hyogo 661-0974, Japan*
E-mail: n.kotobuki@aist.go.jp
[2]*Graduate School of Environmental Studies, Tohoku University, Aoba 20, Aramaki, Aoba-ku, Sendai 980-8579, Japan*
E-mail: ioku@mail.kankyo.tohoku.ac.jp
[3]*Division of Applied Medical Engineering Science, Graduate School of Medicine, Yamaguchi University, 2-16-1 Tokiwadai, Ube, Yamaguchi 755-8611, Japan*

To observe living cell morphology on ceramics by light microscopy, we fabricated a new material—transparent β- tricalcium phosphate (*t*-βTCP) ceramic—for the purpose of serving as a tissue culture substrate. Bone marrow stromal cells (BMSCs) were obtained from rat femora and cultured on both *t*-βTCP ceramic disks and culture grade polystyrene (PS) dishes in an osteogenic medium. After 1 day of culture, cell attachment and spreading on both the *t*-βTCP and PS substrata were equally and clearly detected by ordinary light microscopy. After 14 days of culture, extensive cell growth, alkaline phosphatase (ALP) staining, and bone mineral deposition could be detected on both substrata. In addition, quantitative biochemical analyses revealed high DNA content, ALP activity, and osteocalcin content of these cultures. This experiment is significant in that all of the results were similarly observed on both the *t*-βTCP and PS substrata, indicating the excellent properties of βTCP ceramics for BMSCs culture towards osteogenic differentiation.

Introduction

Viable cells can be cultured in suitable scaffolds, and composites of such cells have already been clinically applied to patients. As examples, some polymers such as collagen combined with a variety of cultured cells are currently being used for cartilage and skin regeneration [1, 2], and ceramics combined with mesenchymal cells are being used for bone regeneration [3]. In our clinical cases, culturing a patient's derived mesenchymal cells on any of hydroxyapatite (HA), β-tricalcium phosphate (βTCP), or alumina ceramics has been used in treating patients having skeletal problems. In particular, before cell transplantation to the patients, we forced the mesenchymal cells to become osteoblasts followed by the formation of bone matrix on a ceramic surface [4, 5]. We have therefore defined the tissue-engineered construct fabricated by culturing mesenchymal cells on ceramics as *regenerative cultured bone tissue* [6].

Many researchers, ourselves included, have previously reported that composites of fresh bone marrow (without culture) and porous HA or βTCP [7–9] can show extensive new bone formation after *in vivo* implantation. We considered that the bone formation could be initiated on a ceramic surface by attaching mesenchymal cells from bone marrow. However, due to *in vivo* conditions, observation of the cells/ceramic interaction is difficult. In this regard, *in vitro* culturing of bone marrow stromal cells (BMSCs) on ceramic disks might be another approach for observing cells/ceramic interaction. Usually, cultured cells can be observed with

*Author to whom all correspondence should be addressed.

0957–4530

an ordinary microscope when the culture is on culture dishes. However, due to the opacity of the ceramics, microscopic observation of the cells on ceramics is very difficult. Scanning electron microscopy (SEM) or other techniques can be used to observe the cells on the ceramics, but these techniques usually require cell fixation by glutaldehyde, paraformaldehyde, or similar fixative solution, and the cells are no longer viable. Moreover, consecutive observation of the same specimen during the culture period is impossible.

If the ceramic were transparent, we could use an ordinary microscope for observation, which would enable us to detect cell attachment, spreading, proliferation, and differentiation cascade. Recently, it has been claimed that transparent ceramics are useful for the observation of cultured cells [10]. Transparent ceramics are mainly made by a spark plasma sintering process (SPS) [11]. SPS systems have many advantages such as rapid sintering, sintering with fewer additives, uniform sintering, low operating expense, and relatively easy operation compared to that of conventional systems using hot press (HP) sintering, hot isostatic pressing (HIP), or atmospheric furnaces.

β-TCP ceramics are known to be highly biodegradable. Porous types of β-TCP have attracted much attention within the field of bone reconstruction [12–15]. The rates of proliferation and differentiation of cultured cells on β-TCP ceramics have been demonstrated by biochemical analyses or gene expression analysis [16, 17] and SEM observation. However the ceramics used were opaque and direct observation was difficult to accomplish. Therefore, whether the surface of the ceramic could support cell attachment, proliferation, and differentiation was not clear. In this study, we made transparent βTCP (t-βTCP) ceramic disks (20 mm in diameter) using the SPS sintering method. We used rat BMSCs as the cell source and observed cell attachment, proliferation, and osteogenic differentiation on the t-βTCP ceramic disks as well as on culture grade polystyrene (PS) dishes as a positive control. PS dishes have been commonly used as cell culture substrates for a long time and their suitability is well known. This report describes not only the morphological but also the biochemical qualitative analyses of the BMSCs culture and includes a comparative study of the culture on t-βTCP and PS.

Materials and methods

Preparation of transparent βTCP (t-βTCP)

A fine powder made of βTCP (Taiheikagaku, Co. Ltd., Japan) was used as the basic material. One gram of this powder was poured into a graphite mold (inner diameter: 15 mm), and then sintered by the spark plasma sintering process (SPS: Dr Sinter-511S, Sumitomo Coal Mining, Tokyo, Japan). The samples were pressed uniaxially under 10 MPa, then heated at 1000 °C for 10 min at a heating rate of 25 °C/min. Each ceramic disk consisted of polycrystalline, transparent materials with a diameter of 20 mm and a thickness of 2 mm. The surface shapes and crystallographic analyses were determined using a scanning electron microscope (SEM, SM-300, Topcon Corporation, Tokyo, Japan) and an X-ray diffractometer (XRD, Geiger flex 2027, Rigaku, Japan), respectively.

Surface characterization

The surface roughness of the t-βTCP ceramic disks and PS dishes was measured by using a profilometer (Surfcorder SE-30D, Kosaka Lab., Ltd.) with a 5-μm tipped diamond stylus. Then, both the average roughness (Ra) and maximum roughness (Rz) were quantified. The sessile contact angles (SCA) of t-βTCP ceramic disks and PS dishes were determined using a Milli-Q water system and a goniometer (Face Contact-Angle Meter, Kyowa Kaimenkagaku Co., Ltd. Tokyo, Japan). A probability (p) of less than 0.05 was considered significant.

Cell culture

The preparation and osteogenic differentiation of bone marrow stromal cells (BMSCs) from 7-week-old male Fischer 344 (F344) rats were performed as described by Maniatopoulos *et al.* [18] with some modifications by us [19]. In brief, rat bone marrow plugs were flushed out and suspended in a culture medium, minimum essential medium (MEM, Nacalai Tesque, Inc., Kyoto, Japan) containing 15% fetal bovine serum (FBS, JRH Biosciences, Inc., KS, USA) and 1% antibiotics. These bone marrow cells were cultured in a humidified atmosphere of 95% air with 5% CO_2 at 37 °C.

The mesenchymal cells, which have osteogenic potentials, were contained in BMSCs. The adherent BMSCs were initially cultured up to 80% confluence in T-75 flasks, harvested, and resuspended to 5×10^5 cells/mL in culture medium using 0.05% trypsin/0.53 mM EDTA. One mL of cell suspension was applied to each sterilized t-βTCP ceramic disk (3.1 cm^2), which were placed into a 12-well PS plate (3.8 cm^2). As a control, the same amount of cell suspension was also applied directly in a PS well having no disks. These cells were cultured with osteogenic medium containing 10 nM dexamethasone (Dex, Sigma-Aldrich Corporation, MO, USA), 10 mM β-glycerophosphate (β-GP, Merck, Darmstadt, Germany), and 0.28 mM ascorbic acid 2-phosphate magnesium salt n-hydrate (AAc, Sigma-Aldrich Corp.). The culture medium was changed two or three times per week. During the culture period, the cell morphologies at different stages of cell attachment, proliferation, and differentiation were observed by light microscopy (Olympus CK41SF, Olympus Optical, Co., Ltd., Tokyo, Japan). Some cultures did not have Dex added but the other conditions were the same as above.

Qualitative biochemical analysis

Alkaline phosphatase (ALP) activity staining

At day 14, the cultured cells on both the *t*-βTCP ceramic disks and the PS dishes were rinsed with phosphate buffer saline (PBS) and fixed with 4% paraformaldehyde for 10 min at 4 °C. The fixed cells were soaked in 0.1% naphthol AS-MX phosphate and 0.1% fast red violet LB salt in 56 mM 2-amino-2-methyl-1, 3-propanediol (pH 9.9) for 10 min at room temperature and then washed with PBS.

Alizarin Red S staining

At day 14, the cultured cells on both the *t*-βTCP ceramic disks and the PS dishes were washed with PBS and fixed with 4% paraformaldehyde for 10 min at 4 °C. The fixed cells were soaked in 0.5% Alizarin red S /PBS for 10 min at room temperature and then washed with PBS. Non-specific reactions were removed by a wash step using 70% ethanol (EtOH). The stain was used to detect calcium in the extracellular matrix. To check a background level of Alizarin Red S, *t*-βTCP ceramic disks without cells were soaked into Alizarin red S in the same condition to cells (Fig. 6(e)).

Calcein uptake

The calcium in the extracellular matrix was also determined by using calcein, which is a calcium-chelating fluorescence chemical [20]. One μg/mL

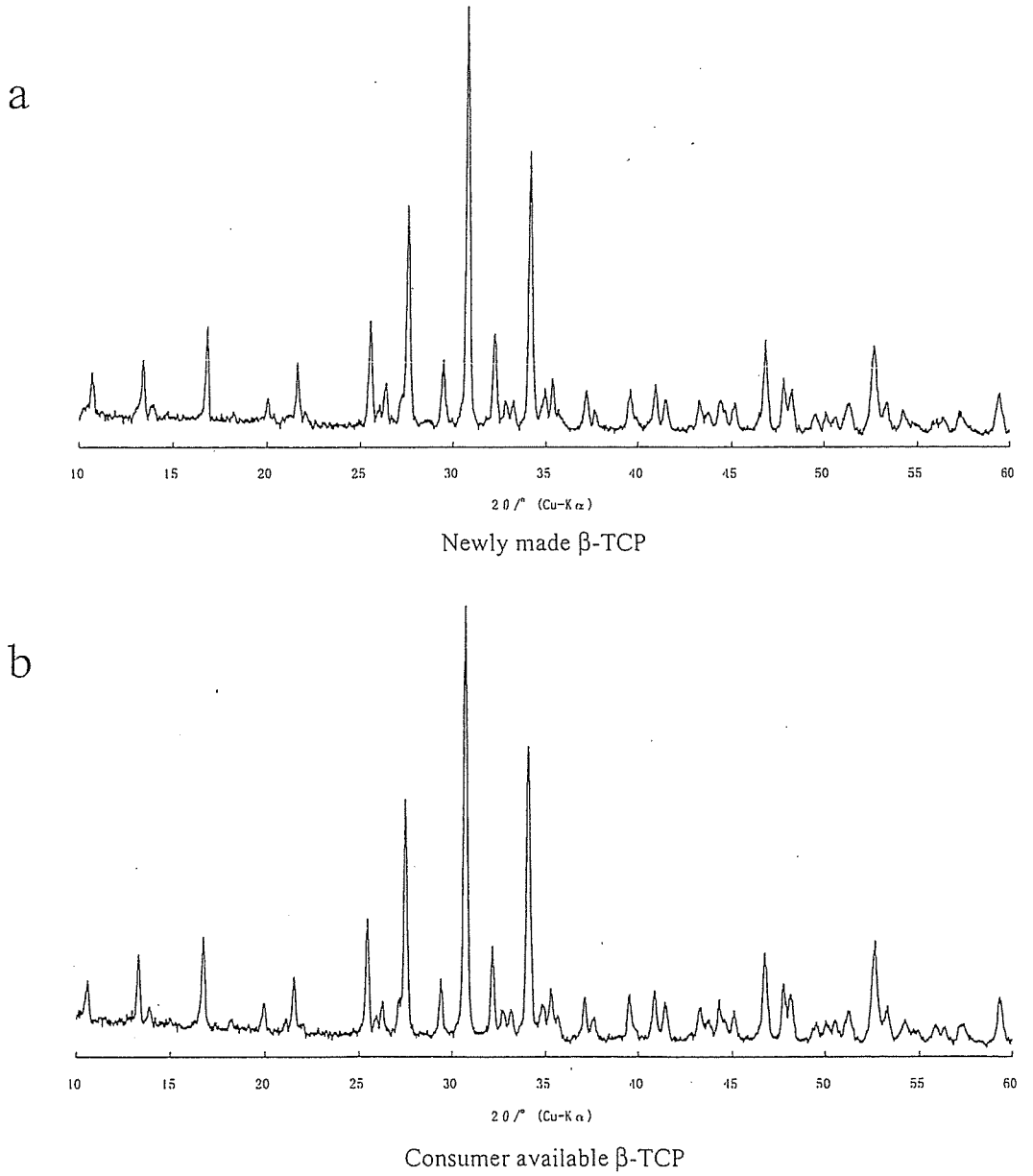

Figure 1 Powder X-ray diffraction (XRD) pattern of transparent βTCP ceramics made by spark plasma sintering (a) and standard βTCP (b). Details are given in the Materials and methods section.

calcein (Dojindo Laboratories, Kumamoto, Japan) was added to the medium during culture. The fluorescence of the incorporated calcein was observed by using a fluorescent microscope (IX70, Olympus). The medium containing calcein was removed and washed with PBS immediately before these analyses. To check a background level of calcein, t-βTCP ceramic disks without cells were soaked into medium containing calcein in the same condition to cells (Fig. 4(e)).

Quantitative biochemical analysis

Measurement of DNA contents

The DNA contents were measured by using Hoechst 33258 and expressed as $\mu g/cm^2$. The cells were scraped off the t-βTCP or PS surface into 0.5 mL of buffer (10 mM Tris-HCl, 1 mM EDTA and 100 mM NaCl (pH 7.4)) and sonicated. 20 μL of suspended cell solution was added to 0.2 mL of buffer containing 5 μg/mL Hoechst 33258 and the fluorescence was measured on a

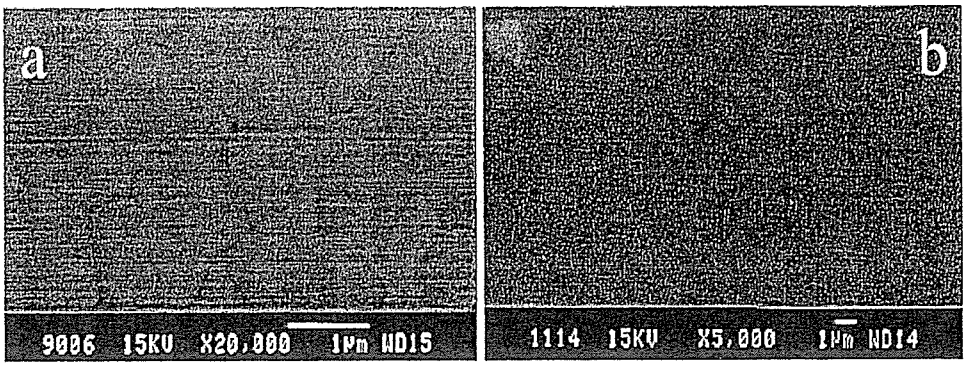

Figure 2 SEM images of transparent βTCP (a) and culture grade polystyrene (PS) (b) Bar: 1 μm. The surface of a culture grade PS dish is very smooth and, therefore, most of the SEM photos were out of focus. To bring the object into focus, we photographed a dish contaminated with a very small dust particle (shown at the upper left) as a pointer.

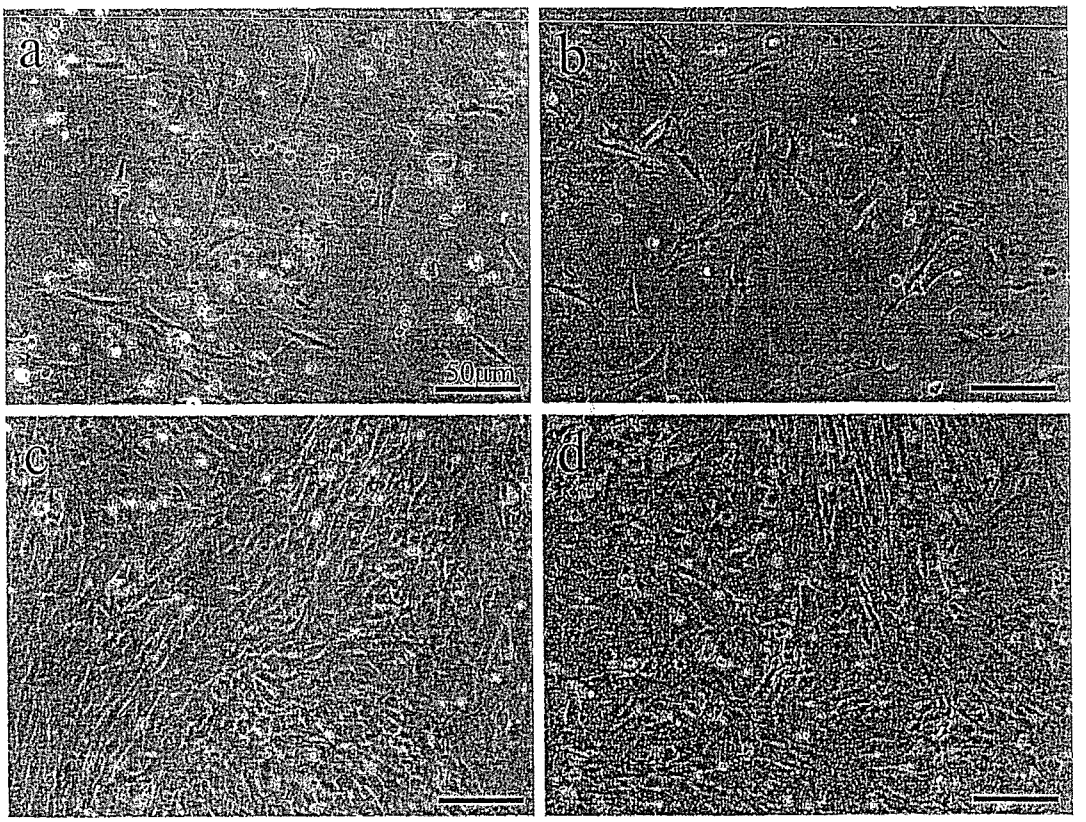

Figure 3 Cell morphology of rat BMSCs seeded on transparent βTCP ceramic disks and culture grade polystyrene (PS) dishes. The cells seeded on βTCP ceramic disks are shown in the left column (a, c). The cells seeded on PS dishes are shown in the right column (b, d). Bar: 50 μm. Cell morphology at day 1 (a, b) and day 4 (c, d) after BMSCs seeding on PS dishes and t-βTCP ceramic disks observed by light microscopy. One day after cell seeding, the cells began to spread on the surface. Cells on both substrata proliferated well and most cells had a fibroblastic shape after 4 days.

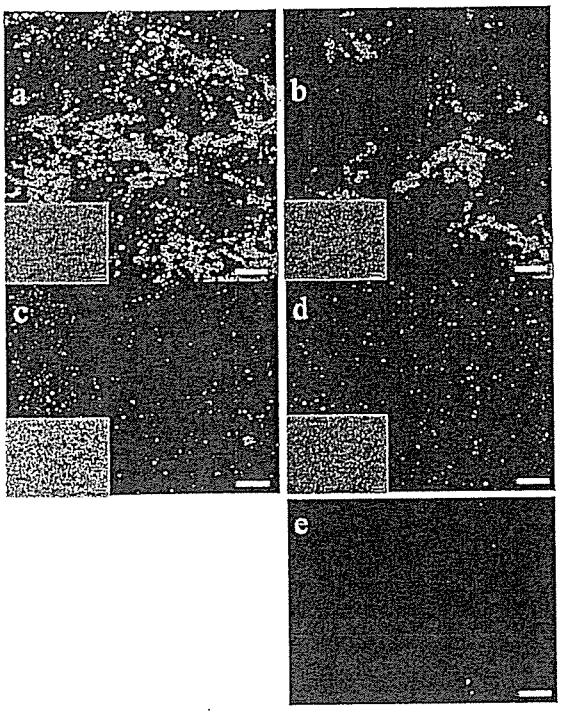

Figure 4 Calcein uptake by rat BMSCs seeded on transparent βTCP ceramic disks and culture grade PS dishes at day 14. Bar: 200 μm. When BMSCs were cultured in the presence of Dex, the culture on both culture grade PS dishes (a) and transparent βTCP (t-βTCP) ceramic disks (b) showed extracellular mineralization indicated by a green fluorescence. In contrast, in the absence of Dex, cells did not differentiate into osteoblasts and the green fluorescence was not detected (c, d). Each inset at lower left shows the phase contrast microscopic view of the corresponding field. Background level of calcein when t-βTCP without cells were soaked into calcein contained medium were shown in e.

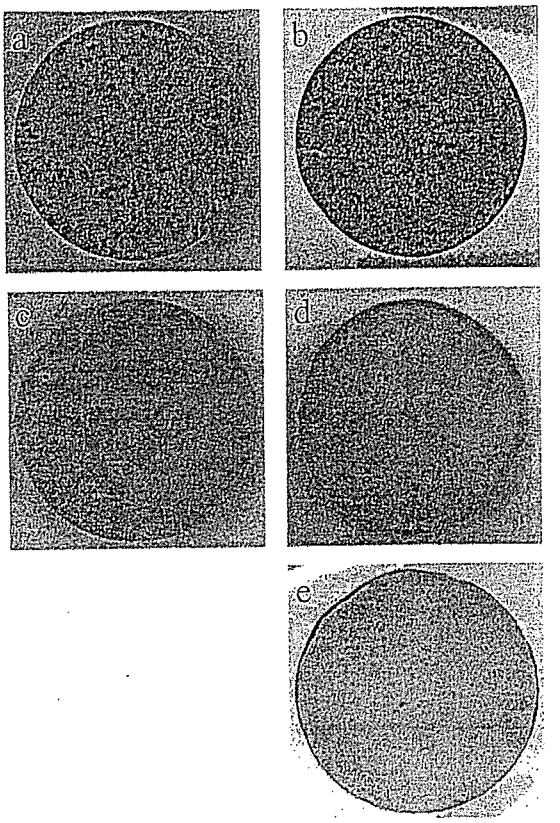

Figure 6 Macroscopic observation of ALP (a, c) and Alizarin Red S staining (b, d). When BMSCs were cultured in the presence of Dex (a, b), the cells on transparent βTCP differentiated into osteoblasts and showed extensive ALP (a) and Alizarin Red S (b) staining over the entire ceramics area compared with the control culture without Dex (c, d). Background level of Alizarin Red S when t-βTCP without cells were soaked into Alizarin Red S were shown in e.

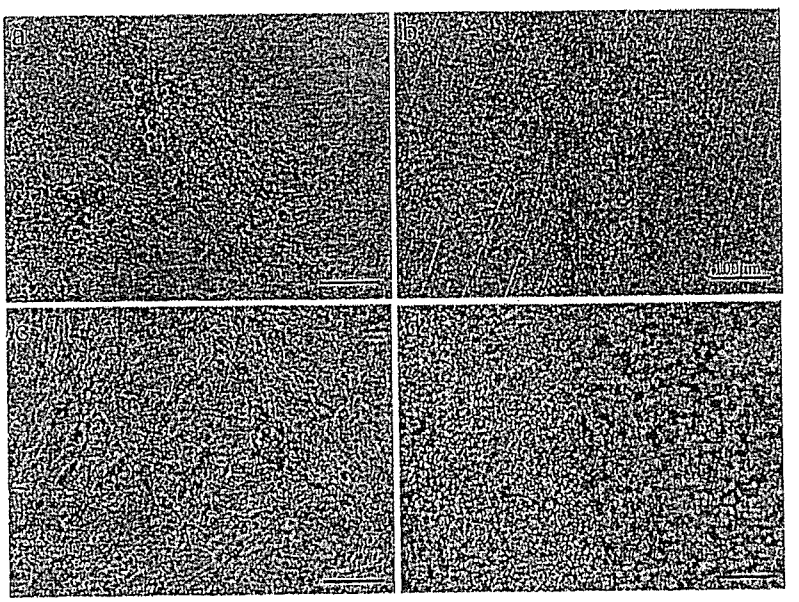

Figure 5 Microscopic observation of ALP and Alizarin Red S staining of the BMSCs culture. Bar: 100 μm. BMSCs were cultured in the presence of Dex for 14 days. Numerous regions of the cultured cells were positive for ALP on both t-βTCP ceramic disks (a) and PS dishes (c). Positive areas are represented in red. Strong Alizarin Red S stain could be detected in many cellular as well as extracellular regions on both the t-βTCP ceramic disks (b) and PS dishes (d).

micro plate reader (Wallac 1420 ARVOsx, PerkinElmer Life & Analytical Sciences, MA, USA). The standard DNA solutions were prepared using salmon sperm DNA (Invitrogen).

Alkaline phosphatase (ALP) activity assay

ALP activity of the cultured cells was examined quantitatively by the specific convention of *p*-nitro phenyl phosphate (pNPP) into *p*-nitro phenol (pNP). The cells were scraped off *t*-βTCP or PS surface into 0.5 mL of 10 mM Tris-HCl, 1 mM EDTA, and 100 mM NaCl (pH 7.4). The suspended cell solution was sonicated and centrifuged at 10,000 ×g for 1 min at 4 °C. An aliquot (20 μL) of the supernatant was assayed for ALP activity using PNPP solution (Zymed Laboratories Inc. CA, USA). The aliquot was incubated at 37 °C for 30 min. After enzymatic reaction was stopped with 0.2 M NaOH, the aliquot was measured for the absorbance of *p*-NP product formed at 405 nm on a micro plate reader (Wallac 1420 ARVOsx). Enzyme activity was expressed as μmol of pNP released/30 min/DNA content.

Measurement of Osteocalcin deposited in extracellular matrix by ELISA

The cells were scraped off and sonicated, then centrifuged at 10000 ×g for 10 min. After treatment of the precipitation in 20% formic acid for 2 days, the samples were centrifuged at 800 ×g for 10 min and the supernatants were subjected to gel filtration to eliminate inorganic ions. Gel-filtered samples were evaporated for concentration. The concentrated samples were added to an EIA plate and immobilized with anti-rat osteocalcin antibody to measure the concentration of osteocalcin with an intact rat osteocalcin EIA kit (Biomedical Technologies Inc. MA, USA). Osteocalcin deposition was expressed as ng/DNA content.

Results

Fig. 1(a) shows the X-ray diffraction (XRD) pattern of a spark plasma sintering (SPS) specimen of *t*-βTCP. The peaks in both figures clearly show that the specimen we made is similar to that of typical βTCP (Fig. 1(b)). We analyzed the surfaces of the *t*-βTCP ceramic disks by scanning electron microscopy (SEM) before the cell culture. Although the surfaces of the *t*-βTCP ceramic disks were slightly rough compared with the surfaces of the PS (Fig. 2(b)), the grain structure of the surface of the sintered *t*-βTCP ceramic disks was fine (less than 1 μm) (Fig. 2(a)).

It is well known that the surface roughness and wettability of culture substrata influence cell attachment and proliferation. The average roughness and maximum roughness of both the *t*-βTCP ceramic disks and the PS dishes were measured by using a profilometer (Table I). The roughness levels of the specimens were similar. We also checked the wettability of the *t*-βTCP ceramic disks and the PS dishes, which is represented by sessile contact angles (SCA) (Table I). The SCA of the *t*-βTCP ceramic disks and the PS dishes showed no significant difference. The results indicate that surface structure is not an important factor in comparing cellular responses on *t*-βTCP ceramic disks to that on PS dishes.

TABLE I Surface roughness and sessile contact angle of each culture substrate

Material	Surface roughness (μm) Ra	Rz	SCA (°±SD)
Culture dish	0.005	0.040	71.0 ± 3.42
β-TCP	0.008	0.079	74.7 ± 3.92

We observed the cell attachment, spreading, and proliferation of rat BMSCs on both culture substrata during the early culture periods. Then, the capacity of BMSCs for osteogenic differentiation was investigated during the late culture periods. The *t*-βTCP ceramic disks are sufficiently transparent to perform microscopic observations and, thus, the cells cultured on the *t*-βTCP ceramic disks can easily be observed by light microscopy equal to those on PS dishes. At a very early stage of the culture, rat BMSCs attached, followed by spreading on not only the PS dishes but also on the *t*-βTCP ceramic disks. One day after the seeding, most of the cells were able to attach and exhibit the morphological characteristics of mesenchymal types (spindle cell morphology) (Fig. 3(a) and (b)). The cells proliferated well and almost all were spindle-shaped after 4 days on both substrata (Fig. 3(c) and (d)). It is thus suggested that rat BMSCs could easily attach, spread, and proliferate on *t*-βTCP ceramics as well as on PS.

In order to analyze the osteogenic differentiation of BMSCs, the BMSCs were further cultured on both *t*-βTCP ceramic disks and PS dishes in the presence of dexamethasone (Dex) for 14 days, and cell morphology was observed by light microscopy. Dex is used because it is well known as an osteogenic factor. To observe the extracellular mineralized matrix more clearly, we added calcein to the medium and measured its fluorescent intensity. When cultured in the osteogenic condition for 14 days, the same level of mineralized bone matrix on both the *t*-βTCP ceramic disks and the PS dishes was observed (Fig. 4(a) and (b)). In contrast, the BMSCs cultured in the absence of Dex showed no osteoblastic cell shape but did show a fibroblastic shape and no evidence of matrix formation (Fig. 4(c) and (d)). These findings indicate that BMSCs can easily differentiate into osteoblasts on the surface of *t*-βTCP ceramics, resulting in the formation of bone matrix under osteogenic

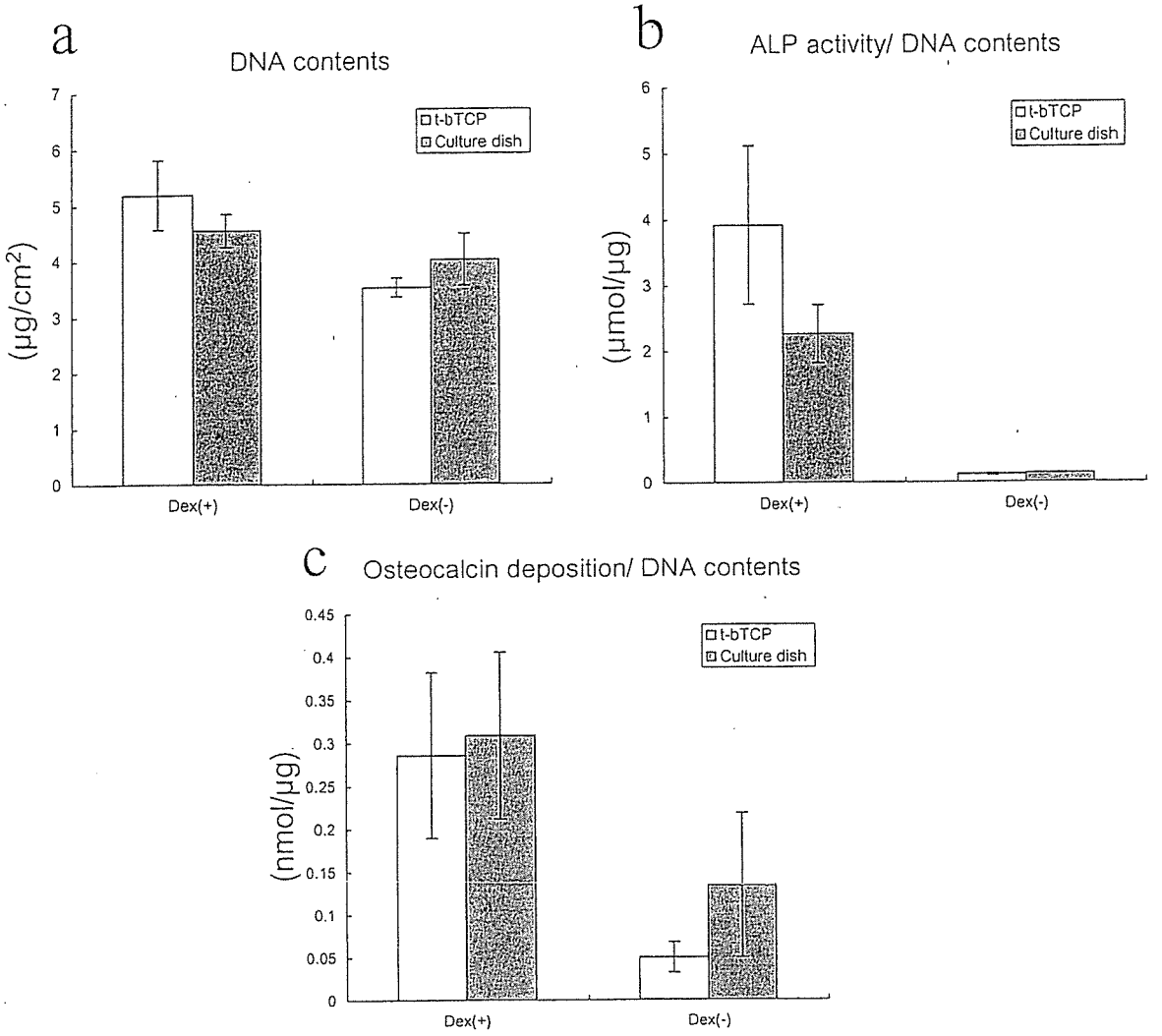

Figure 7 Quantitative and biochemical analyses of BMSCs cultured in the presence (+) or absence (−) of Dex. BMSCs were cultured on both transparent βTCP ceramic disks (t-βTCP) and culture grade polystyrene dishes (culture dish) for 14 days. The DNA contents were represented as micrograms per cm^2 (a). ALP activity (b) and osteocalcin deposition (c) were normalized for DNA content.

conditions. Importantly, the cascade of the differentiation of BMSCs can equally be observed on both t-βTCP ceramics and PS.

To confirm the osteogenic differentiation of BMSCs on the t-βTCP ceramic disks, we performed alkaline phosphatase (ALP) activity and Alizarin Red S staining after two weeks of cultivation. ALP, which is a cell surface protein, is known as an early marker for osteoblastic differentiation and Alizarin Red S can identify calcium in the matrix. Many clusters of cells were well stained with ALP on both the t-βTCP ceramic disks (Fig. 5(a)) and PS dishes (Fig. 5(c)) when cultured with Dex. As seen in the ALP stain, the cultures with Dex were strongly stained with Alizarin Red S (Fig. 5(b) and (d)). In contrast, the cultures without Dex were barely stained with either ALP or Alizarin Red S, as evidenced by macroscopic observation (Fig. 6). These biochemical data showed that the osteogenic differentiation of BMSCs cultured in the presence of Dex could occur on both t-βTCP ceramic and PS substrata.

After 14 days of culture, the DNA contents from each substrate were measured. The DNA contents were similar regardless of the culture substrata (Fig. 7(a)). As seen in ALP staining (Figs. 5 and 6) the cultures on both substrata with Dex showed high ALP activity compared with the culture without Dex (Fig. 7(b)). These data confirmed the morphological data (Figs. 3–6) that βTCP ceramics as well as PS supports the proliferation and osteogenic differentiation of BMSCs cultured in the presence of Dex. To confirm the osteogenic differentiation, we measured the bone-specific protein of osteocalcin. As seen in Fig. 7(C), high levels of osteocalcin were detected in the culture with Dex on both substrata. These quantitative biochemical data were evidence that the surfaces of both the t-βTCP ceramic disks and the PS dishes provide considerable

support for the osteoblastic differentiation cascade of BMSCs.

Discussion

In this study, cell behavior on transparent βTCP ceramic disks was compared with that on culture grade PS dishes. PS dishes are considered the gold standard substratum for cell cultivation and were therefore used in the present experiment as a positive control. It has also been reported that the surface characteristics of the culture substrata affect cell behavior during the culture period [21, 22]. As can be seen in Table I, the surface roughness and wettability of t-βTCP were similar to those of PS. It is considered that the optimum wettability for cell attachment is about 70° (defined by sessile contact angle; SCA), and the SCA of t-βTCP as well as PS is nearly 70°. Additionally, the surface of t-βTCP is very smooth as is that of PS as observed by SEM (Fig. 2). These data mean that the wettability of t-βTCP is suitable for cell attachment and that surface roughness is not a decisive factor for comparing cell behavior on both substrata.

Currently, *in vitro* osteogenic differentiation on the various ceramics can be monitored by ALP staining or calcium staining after fixation as shown in Fig. 6. However, microscopic observation of this staining is difficult due to the opacity of ordinary ceramics. In addition, staining cannot be used for repeated monitoring of the same specimen during the culture period. In this regard, by using t-βTCP ceramic, we can detect the ALP and Alizarin Red S stain at the cellular level (Fig. 5). By adding calcein to the culture medium, we can clearly monitor the differentiation indicated by fluorescence emission (Fig. 4). Fluorescence can be detected repeatedly for the same specimen during the entire culture period. As seen in the results, we confirmed the capability of t-βTCP to enable BMSCs attachment, proliferation (Fig. 3), and osteogenic differentiation as confirmed by ALP stain, Alizarin Red S stain (Fig. 5), and calcein uptake (Fig. 4). We also confirmed that the capability of t-βTCP as a cell culture substrate was similar to that of PS. The qualitative analyses were confirmed by quantitative analyses of DNA, ALP activity, and osteocalcin measurements (Fig. 7). The data verify that the surface of t-βTCP ceramic is equivalent to that of culture-grade PS and has the capability of supporting cellular adhesion and proliferation, which results in the osteogenic differentiation of BMSCs. It is important to demonstrate a functional equivalence of both substrata because PS is suitable to *in vitro* culture but the appropriate materials for tissue engineering is βTCP. It is possible to make various type of βTCP combined with extracellular matrix or growth factors. And we can control a composition of βTCP. Together, we concluded that an observable transparent βTCP is useful materials for *in vitro* research in the field of medicine especially tissue engineering.

Conclusion

We fabricated a new material, a transparent βTCP (t-βTCP) ceramic, and used it as a culture substrate. The ceramic material enables the observation of cultured cells by light microscopy. The shape of the cells on the ceramic disks was as clearly detected as that seen on culture grade polystyrene (PS) dishes. In this report, rat bone marrow stromal cells (BMSCs) were cultured. As a result, cell attachment, proliferation, and differentiation of BMSCs on t-βTCP disks were similar to those on (PS) dishes. The results were confirmed by quantitative biochemical assay. All results confirmed the excellent properties of βTCP for supporting the differentiation capability of BMSCs, which resulted in osteoblastic phenotype expression.

Acknowledgments

We thank our colleagues at the National Institute of Advanced Industrial Science and Technology (AIST), at the Graduate School of Environmental Studies, Tohoku University, and at the Graduate School of Medicine, Yamaguchi University. And we especially thank Dr. Oshimura at the Graduate School of Medical Sciences, Tottori University for valuable discussion. The Three-Dimensional Tissue Module Project of METI (a Millennium Project) and Grant-in-Aid for Scientific Research Japan supported this work.

References

1. S. WAKITANI, K. IMOTO, T. YAMAMOTO, M. SAITO, N. MURATA and M. YONEDA, *Osteoarthritis Cartilage* **10** (2002) 199.
2. M. OCHI, Y. UCHIO, K. KAWASAKI, S. WAKITANI and J. IWASA, *J. Bone Joint Surg. Br.* **84** (2002) 571.
3. R. QUARTO, M. MASTROGIACOMO, R. CANCEDDA, S. M. KUTEPOV, V. MUKHACHEV, A. LAVROUKOV, E. KON and M. MARCACCI, *N. Engl. J. Med.* **344** (2001) 385.
4. H. OHGUSHI and A. I. CAPLAN, *J. Biomed. Mater. Res.* **48** (1999) 913.
5. H. OHGUSHI, J. MIYAKE and T. TATEISHI, *Novartis Found Symp.* **249** (2003) 118.
6. N. KOTOBUKI, M. HIROSE, Y. TAKAKURA and H. OHGUSHI, *Artif. Organs* **28** (2004) 33.
7. H. OHGUSHI, M. OKUMURA, S. TAMAI, E. C. SHORS and A. I. CAPLAN, *J. Biomed. Mat. Res.* **24** (1990) 1563.
8. H. OHGUSHI, M. OKUMURA, T. YOSHIKAWA, K. INOUE, N. SENPUKE and S. TAMAI, *ibid.* **26** (1992) 885.
9. T. UEMURA, J. DONG, Y. WANG, H. KOJIMA, T. SAITO, D. IEJIMA, M. KIKUCHI, J. TANAKA and T. TATEISHI, *Biomaterials.* **24** (2003) 2277.
10. N. KOTOBUKI, K. IOKU, D. KAWAGOE, H. FUJIMORI, S. GOTO and H. OHGUSHI, *ibid.* (in press)
11. K. IOKU, D. KAWAGOE, H. TOYA, H. FUJIMORI, S. GOTO, K. ISHIDA, A. MIKUNI and H. MAE, *Trans. Mater. Res. Soc. Japan* **27** (2002) 447.

12. K. OHURA, M. BOHNER, P. HARDOUIN, J. LEMAITRE, G. PASQUIER and B. FLAUTRE, *J. Biomed. Mater. Res.* 30 (1996) 193.
13. K. OHSAWA, M. NEO, H. MATSUOKA, H. AKIYAMA, H. ITO, H. KOHNO and T. NAKAMURA, *ibid.* 52 (2000) 460.
14. K. KURASHIMA, H. KURITA, Q. WU, A. OHTSUKA and H. KOBAYASHI, *Biomaterials* 23 (2002) 407.
15. M. SAITO, H. SHIMIZU, M. BEPPA and M. TAKAGI, *J. Orthop. Sci.* 5 (2000) 275.
16. P. KASTEN, R. LUGINBUHL, M. VAN GRIENSVEN, T. BARKHAUSEN, C. KRETTEK, M. BOHNER and U. BOSCH, *Biomaterials* 24 (2003) 2593.
17. U. MAYR-WOHLFART, J. FIEDLER, K. P. GUNTHER, W. PUHL and S. KESSLER, *J. Biomed. Mater. Res.* 57 (2001) 132.
18. C. MANIATOPOULOS, J. SODEK and A. H. MELCHER, *Cell Tissue Res.* 254 (1988) 317.
19. M. IKEUCHI, Y. DOHI, K. HORIUCHI, H. OHGUSHI, T. NOSHI, T. YOSHIKAWA, K. YAMAMOTO and M. SUGIMURA, *J. Biomed. Mater. Res.* 60 (2002) 61.
20. E. UCHIMURA, H. MACHIDA, N. KOTOBUKI, T. KIHARA, S. KITAMURA, M. IKEUCHI, M. HIROSE, J. MIYAKE and H. OHGUSHI, *Calcif. Tissue Int.* 73 (2003) 575.
21. G. KHANG, J. W. LEE, J. H. JEON, J. H. LEE and H. B. LEE, *Biomaterials Res.* 1 (1997) 1.
22. T. U. YUKOSHI and T. MATSUDA, *Langmuir* 11 (1995) 4135.

Received 19 August 2004
and accepted 25 May 2005

Available online at www.sciencedirect.com
ScienceDirect
ELSEVIER
Biochemical and Biophysical Research Communications 349 (2006) 1242–1249
BBRC
www.elsevier.com/locate/ybbrc

Beraprost sodium enhances neovascularization in ischemic myocardium by mobilizing bone marrow cells in rats

Yoshinori Miyahara [a], Shunsuke Ohnishi [a], Hiroaki Obata [a], Kozo Ishino [b], Shunji Sano [b], Hidezo Mori [c], Kenji Kangawa [d], Soichiro Kitamura [e], Noritoshi Nagaya [a,*]

[a] *Department of Regenerative Medicine and Tissue Engineering, National Cardiovascular Center Research Institute, Osaka, Japan*
[b] *Department of Cardiovascular Surgery, Okayama University Graduate School of Medicine, Dentistry and Pharmaceutical Sciences, Okayama, Japan*
[c] *Department of Cardiac Physiology, National Cardiovascular Center Research Institute, Osaka, Japan*
[d] *Department of Biochemistry, National Cardiovascular Center Research Institute, Osaka, Japan*
[e] *Department of Cardiovascular Surgery, National Cardiovascular Center, Osaka, Japan*

Received 13 August 2006
Available online 7 September 2006

Abstract

Beraprost sodium, an orally active prostacyclin analogue, has vasoprotective effects such as vasodilation and antiplatelet activities. We investigated the therapeutic potential of beraprost for myocardial ischemia. Immediately after coronary ligation of Sprague–Dawley rats, beraprost (200 μg/kg/day) or saline was subcutaneously administered for 28 days. Four weeks after coronary ligation, administration of beraprost increased capillary density in ischemic myocardium, decreased infarct size, and improved cardiac function in rats with myocardial infarction. Beraprost markedly increased the number of CD34-positive cells and c-kit-positive cells in plasma. Also, four weeks after coronary ligation of chimeric rats with GFP-expressing bone marrow, bone marrow-derived cells were incorporated into the infarcted region and its border zone. Treatment with beraprost increased the number of GFP/von Willebrand factor-double-positive cells in the ischemic myocardium. These results suggest that beraprost has beneficial effects on ischemic myocardium partly by its ability to enhance neovascularization in ischemic myocardium by mobilizing bone marrow cells.

Keywords: Prostacyclin analogue; Myocardial infarction; Neovascularization; Bone marrow mobilization

Interruption of myocardial blood flow leads to rapid death of cardiomyocytes and vascular structures, resulting in the development of heart failure [1]. Stem or progenitor cells are mobilized from bone marrow into the peripheral blood in response to tissue ischemia, migrate to sites of injured tissues, and differentiate into endothelial cells and cardiomyocytes [2–4]. However, the compensatory mechanisms are insufficient to heal infarcted myocardium. Earlier studies have shown that bone marrow cells artificially mobilized by cytokines repair the infarcted heart and improve cardiac function after acute myocardial infarction [5,6]. Therefore, enhancement of bone marrow cell mobilization leading to neovascularization following revascularization would be beneficial for the treatment of acute myocardial infarction.

Beraprost sodium (BPS) is a chemically stable prostacyclin analogue owing to its cyclo-pentabenzofuranyl structure [7]. It has been well established that BPS has vasoprotective effects such as vasodilation and antiplatelet activities [8–11]. Thus, BPS has been used in the treatment of peripheral arterial disease [12,13] and pulmonary arterial hypertension [14,15]. Although a limited number of studies suggest therapeutic potential of prostacyclin for the treatment of myocardial ischemia [16–18], the underlying mechanisms still remain unclear. In addition, little information is available regarding the therapeutic potential of prostacyclin analogues such as BPS for myocardial ischemia. A recent study has shown that BPS activates endothelial

* Corresponding author. Fax: +81 6 6833 9865.
E-mail address: nnagaya@ri.ncvc.go.jp (N. Nagaya).

0006-291X/$ - see front matter © 2006 Elsevier Inc. All rights reserved.
doi:10.1016/j.bbrc.2006.08.178

nitric oxide synthase (eNOS) through the c-AMP/protein kinase A pathway [19]. Activation of eNOS is known to contribute to bone marrow cell mobilization, leading to neovascularization [20]. These results raise the possibility that BPS may have beneficial effects on the ischemic myocardium through enhancement of bone marrow cell mobilization.

Thus, the purposes of this study were: (1) to examine the effect of BPS on mobilization and recruitment of bone marrow cells after acute myocardial infarction, (2) to investigate whether BPS induces neovascularization in the ischemic myocardium, and (3) to investigate whether treatment with BPS improves cardiac function in rats with myocardial infarction.

Methods

Model of myocardial infarction. We used male Sprague–Dawley rats (Japan SLC Inc., Hamamatsu, Japan) weighing 185–215 g. Myocardial infarction was produced by left coronary ligation, as described previously [21]. Briefly, after rats were anesthetized with sodium pentobarbital (30 mg/kg), they were artificially ventilated with a volume-regulated respirator. The heart was exposed via a left thoracotomy incision. Then, the left coronary artery was ligated 2–3 mm from its origin between the pulmonary artery conus and the left atrium with a 6-0 Prolene suture. Finally, the heart was restored to its normal position, and the chest was closed. Experimental protocols were performed in accordance with the "Guidelines of the Animal Care Ethics Committee of the National Cardiovascular Center Research Institute", which complies NIH Guidelines.

Administration of BPS. Immediately after coronary ligation, BPS (200 μg/kg/day, Astellas Pharma Inc., Tokyo, Japan) was subcutaneously administered to surviving rats using an osmotic mini-pump for 4 weeks (BPS group, $n = 12$). As a control, saline was similarly administered to rats receiving coronary ligation (Control group, $n = 12$).

Echocardiographic studies. Echocardiographic studies were performed 4 weeks after coronary ligation. M-mode tracings were obtained at the level of the papillary muscles using an echocardiographic system equipped with a 7.5-MHz phased-array transducer (HP SONOS 5500; Hewlett Packard Co., Andover, MA). Anterior and posterior end-diastolic and end-systolic wall thickness, LV end-diastolic and end-systolic dimensions, and LV fractional shortening were measured by the American Society for Echocardiography leading-edge method in three consecutive cardiac cycles. LV meridional wall stress was estimated as $0.344 \times \text{LV pressure} \times \{\text{LV dimension}/(1 + \text{PWT/LV dimension})\}$, where PWT is posterior wall thickness [22].

Hemodynamic studies. Hemodynamic studies were performed 4 weeks after coronary ligation, following echocardiography. After anesthesia with pentobarbital sodium, a 1.5F micromanometer-tipped catheter (Millar Instruments Inc., Houston, TX) was advanced into the LV through the right common carotid artery. Hemodynamic variables were measured with a pressure transducer connected to a polygraph. After completion of these measurements, the left and right ventricles and the lungs were excised and weighed. Infarct size was determined as a percentage of the entire LV area ($n = 5$ in each group), as reported previously [23]. Briefly, incisions were made in the posterior LV so that the tissue could be pressed flat. The circumference of the entire flat LV and of the visualized infarcted area, as judged from both the epicardial and endocardial sides, was outlined on a clear plastic sheet. The difference in weight between the two marked areas on the sheet was used to determine infarct size and was expressed as a percentage of LV surface area.

Measurement of plasma ANP level. Blood samples were obtained 4 weeks after coronary ligation. Plasma atrial natriuretic peptide (ANP), a marker for heart failure, was measured by enzyme immunoassay (Peninsula Laboratories Inc., San Carlos, CA).

Mononuclear cell mobilization and FACS analysis. To investigate whether administration of BPS mobilizes bone marrow cells, an additional 12 rats were randomized to receive BPS (200 μg/kg/day, BPS group, $n = 6$) or saline (Control group, $n = 6$). On the third day of BPS or saline treatment, 4 ml of blood was drawn from the inferior vena cava of each rat. Peripheral blood was obtained at the end of infusion. After mononuclear cells were counted, they were incubated for 30 min at 4 °C with fluorescein isothiocyanate (FITC)-conjugated mouse monoclonal antibodies against rat CD34 (clone ICO-115, Santa Cruz) and CD45 (clone OX-1), and FITC-conjugated rabbit anti-rat c-Kit polyclonal antibody (clone C-19, Santa Cruz). Immunofluorescence-labeled cells were analyzed by quantitative flow cytometry with a FACSCalibur flow cytometer (BD Biosciences, Mountain View, CA). Isotype-identical antibodies served as controls.

RT-PCR assay. To investigate whether bone marrow cells express the prostacyclin receptor (IP receptor), we analyzed expression of its mRNA by reverse transcription-polymerase chain reaction (RT-PCR). In brief, total RNA of bone marrow cells was extracted with guanidine isothiocyanate (RNeasy Mini Kit, Qiagen). Then, reverse-transcribed single-stranded cDNA was subjected to PCR (PCR Amplification Kit, Takara) using primer sets for the IP receptor (Hokkaido System Science Co., Ltd., Sapporo, Japan, forward, 5′-GGCACGAGAGGATGAAGTTTACC-3′; reverse, 5′-GTCAGAGGCACAGCAGTCAATGG-3′) and G3PDH (Clonetech Laboratories Inc., Mountain View, CA, forward, 5′-TGAAGGTCGGTGTCAACGGATTTGGC-3′; reverse, 5′-CATGTAGGCCATGAGGTCCACCAC-3′).

Creation of bone marrow-chimeric rats. To assess recruitment of bone marrow cells after BPS administration, bone marrow transplantation was performed by using male normal Sprague–Dawley rats as recipients and male Green fluorescent protein (GFP)-transgenic rats (SD-Tg [Act-EGFP] CZ-004Osb, Japan SLC Inc.) as donors, using a previously described method [24]. Briefly, bone marrow was harvested by flushing the cavity of femurs and tibias from GFP-transgenic rats with phosphate-buffered saline. Then, 3×10^7 GFP-positive bone marrow cells were individually administered to 12 lethally irradiated (9.0 Gray) rats via the tail vein. Four weeks after transplantation, flowcytometric analysis determined that 90% of peripheral blood mononuclear cells from both donors and 8 of 12 chimeric rats were GFP-positive, suggesting the establishment of stable chimerism. These chimeric rats were subjected to left coronary ligation, followed by administration of BPS (200 μg/kg/day, BPS group, $n = 4$) or saline (Control group, $n = 4$) using an osmotic mini-pump for 4 weeks.

Histological examination. To detect fibrosis in the cardiac muscle, the LV myocardium ($n = 5$, each group) was fixed in 10% formalin, cut transversely in three sections, embedded in paraffin, and stained with Masson's trichrome. To detect capillary endothelial cells in the peri-infarct area, we performed DAB staining (LSAB2 System HRP, Dako Cytomation Co., Denmark) using rabbit polyclonal anti-von Willebrand factor (vWF) antibody (Dako). A total of 10 different fields from three different sections were randomly selected, and the number of capillaries was counted in the peri-infarct area using a light microscope at 200× magnification. Capillary density was expressed as the mean number of capillaries per square millimeter. Also, 4 weeks after coronary ligation in bone marrow-chimeric rats ($n = 4$ in each group), the LV myocardium was excised, embedded in OCT compound, snap-frozen in liquid nitrogen, and cut transversely into 6-μm-thick sections from base to apex. Immunofluorescent staining was performed using rabbit polyclonal anti-vWF antibody (Dako), mouse monoclonal anti-cardiac troponin T antibody (Neomarkers, Fremont, CA), and rabbit polyclonal Alexa-488-conjugated anti-GFP antibody (Molecular Probes Inc., Eugene, OR). The nuclei were counterstained with 4′,6′-diamidino-2-phenylindole (DAPI). We measured the number of GFP/vWF-double-positive cells incorporated into vascular structures in 10 randomly selected fields in the peri-infarct area per section in a blinded fashion using a fluorescence microscope.

Statistical analysis. Numerical values are expressed as means ± S.E.M. Comparisons of parameters between two groups were made by unpaired Student's t test. A value of $p < 0.05$ was considered significant.

Results

Cardiac structure

Body weight at 4 weeks after coronary ligation was significantly greater in the BPS group than in the Control group (Table 1). Right ventricular weight and lung weight in the BPS group were significantly smaller than those in the Control group, although LV weight did not differ between the two groups. Moderate to large infarcts were observed in the Control group (Fig. 1A). However, administration of BPS significantly decreased infarct size in rats with myocardial infarction (Fig. 1A and B). BPS significantly decreased LV end-diastolic dimension (LVDD) (Fig. 1C).

Table 1
Physiological profiles of experimental groups

	Control	BPS
Number	12	12
Body weight (g)		
Baseline	198 ± 3	204 ± 3
After treatment	319 ± 6	352 ± 9*
LV wt/body wt (g/kg)	2.28 ± 0.04	2.27 ± 0.04
RV wt/body wt (g/kg)	0.99 ± 0.05	0.61 ± 0.02**
Lung wt/body wt (g/kg)	6.55 ± 0.62	3.88 ± 0.1**
Plasma AND level (pg/ml)	798 ± 99	498 ± 57*

Control, infarct rats without treatment; BPS, infarct rats treated with BPS administration; AND, atrial natriuretic protein. Data are expressed as means ± SEM. $^{*}p < 0.05$, $^{**}p < 0.01$ vs. Control group.

Cardiac function

Neither heart rate nor mean arterial pressure differed between the BPS and Control groups (Table 2). LV fractional shortening and LV maximum dP/dt in the BPS group were significantly greater than those in the Control group (Fig. 2A and B). LV end-diastolic pressure (LVEDP) in the BPS group was significantly lower than that in the Control group (Fig. 2C). LV minimum dP/dt was also improved by BPS (Fig. 2D). Treatment with BPS attenuated the increase in plasma ANP level after myocardial infarction (Table 1). BPS significantly increased anterior wall thickening, although it did not significantly alter posterior wall thickening (Table 2). Thickness of the anterior and posterior walls tended to be greater in the BPS group, but these changes did not reach statistical significance. LV diastolic wall stress in the BPS group was significantly lower than that in the Control group.

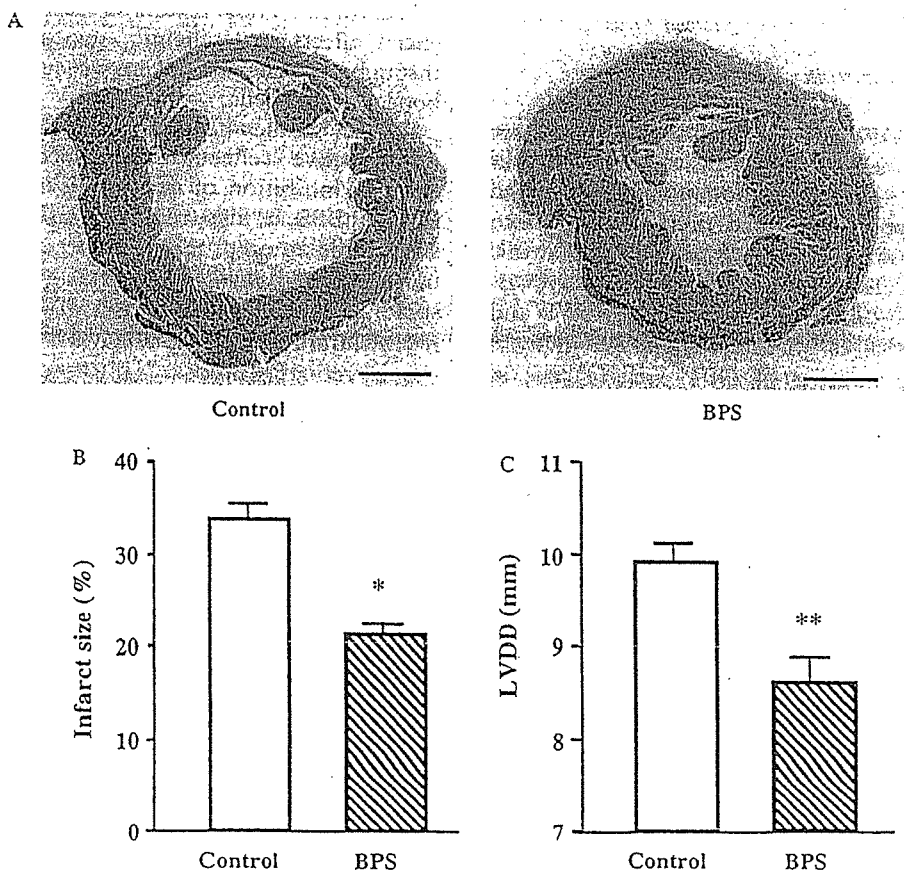

Fig. 1. (A) Representative examples of Masson's trichrome staining of transverse sections of LV myocardium 4 weeks after coronary ligation. Scale bars = 2 mm. (B,C) Quantitative analysis of infarct size and LV end-diastolic dimension (LVDD). Infarcted area and LVDD in the BPS group were significantly smaller than those in the Control group. Data are expressed as means ± SEM. $^{*}p < 0.05$, $^{**}p < 0.01$ vs. Control group.

Table 2
Echocardiographic and hemodynamic data

	Control	BPS
AWT diastole (mm)	0.62 ± 0.04	0.74 ± 0.05
AW thickening (%)	17 ± 3	34 ± 6*
PWT diastole (mm)	1.55 ± 0.07	1.70 ± 0.04
PW thickening (%)	43 ± 4	49 ± 3
Heart rate (bpm)	458 ± 7	471 ± 10
Mean arterial pressure (mmHg)	103 ± 5	115 ± 4
LV systolic pressure (mmHg)	113 ± 4	127 ± 5*
LV diastolic wall stress (kdyne/cm^2)	24 ± 4	5 ± 1**
LV systolic wall stress (kdyne/cm^2)	267 ± 18	225 ± 14

AWT, anterior wall thickness; AW, anterior wall; PWT, posterior wall thickness; PW, posterior wall. Data are expressed as means ± SEM. *$p < 0.05$, **$p < 0.01$ vs. Control group.

Mobilization of bone marrow cells

RT-PCR demonstrated that IP receptor mRNA was expressed in bone marrow cells (Fig. 3A), indicating a direct effect of BPS on these cells. Three-day administration of BPS significantly increased the number of peripheral blood mononuclear cells compared to saline administration (Fig. 3B). Administration of BPS markedly increased the number of circulating progenitor cells such as CD34-positive cells and c-kit-positive cells (Fig. 3C and D). BPS also increased the number of CD45-positive hematopoietic lineage cells (Fig. 3E).

BPS-induced neovascularization

Chimeric rats with GFP-expressing bone marrow were used to assess recruitment of bone marrow cells. Four weeks after coronary ligation, bone marrow-derived GFP-positive cells were incorporated predominantly into the infarcted region and its border zone (Fig. 4A), while these cells were rarely detected in the noninfarcted myocardium. Some of the GFP-positive cells stained for vWF and formed vascular structures. Semi-quantitative analysis demonstrated that the number of GFP-positive cells in the myocardium was significantly greater in the BPS group than in the Control group (Fig. 4B). The number of GFP vWF double-positive cells (bone marrow-derived endothelial cells) in the ischemic myocardium was significantly greater in the BPS group than in the Control group (Fig. 4C). In addition, a small number of GFP-troponin T-double-positive cells were observed in the BPS group (Fig. 4D).

Capillary density

In the peri-infarct area, clustering of relatively small vessels was seen in BPS-treated hearts, which is indicative of recent endothelial regeneration (Fig. 5A). Semi-quantitative analysis also demonstrated that administration of BPS significantly increased the capillary density in the peri-infarct area compared to the Control group (Fig. 5B).

Discussion

In the present study, we demonstrated that treatment with BPS (1) decreased infarct size and improved cardiac structure and function in rats with acute myocardial infarction, (2) increased the number of circulating progenitor cells such as CD34-positive cells and c-kit-positive cells in rats, and (3) increased the number of bone marrow-derived endothelial cells and the capillary density in the ischemic myocardium. These results suggest that BPS may have beneficial effects on ischemic myocardium at least in part through enhancement of neovascularization by mobilizing bone marrow cells.

Earlier studies have reported that prostacyclin has cardioprotective effects in ischemia–reperfusion injury through inhibition of neutrophil activation and migration [25,26]. BPS is also reported to inhibit chemotaxis and superoxide anion production of neutrophils which contribute to tissue damage by releasing tissue destructive lysosomal enzymes [27]. Infusion of BPS has been shown to reduce infarct size in the dog heart with left coronary occlusion by reducing myocardial oxygen demand and by inhibition of the migration of neutrophils [28]. However, these

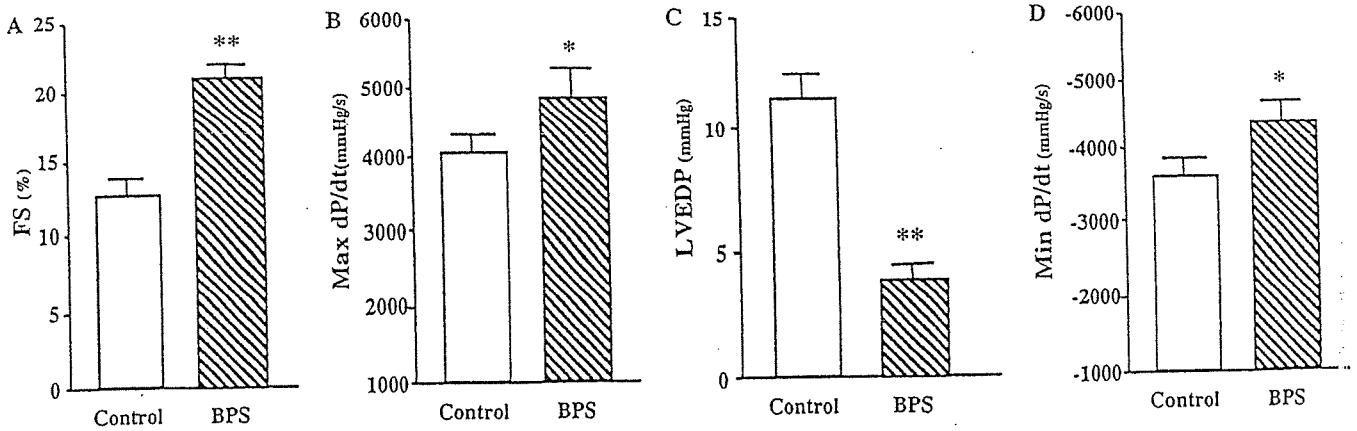

Fig. 2. Cardioprotective effects of BPS on echocardiographic and hemodynamic parameters. FS, fractional shortening; LVEDP, LV end-diastolic pressure; Max and Min dP/dt, maximum and minimum dP/dt. Data are expressed as means ± SEM. *$p < 0.05$, **$p < 0.01$ vs. Control group.

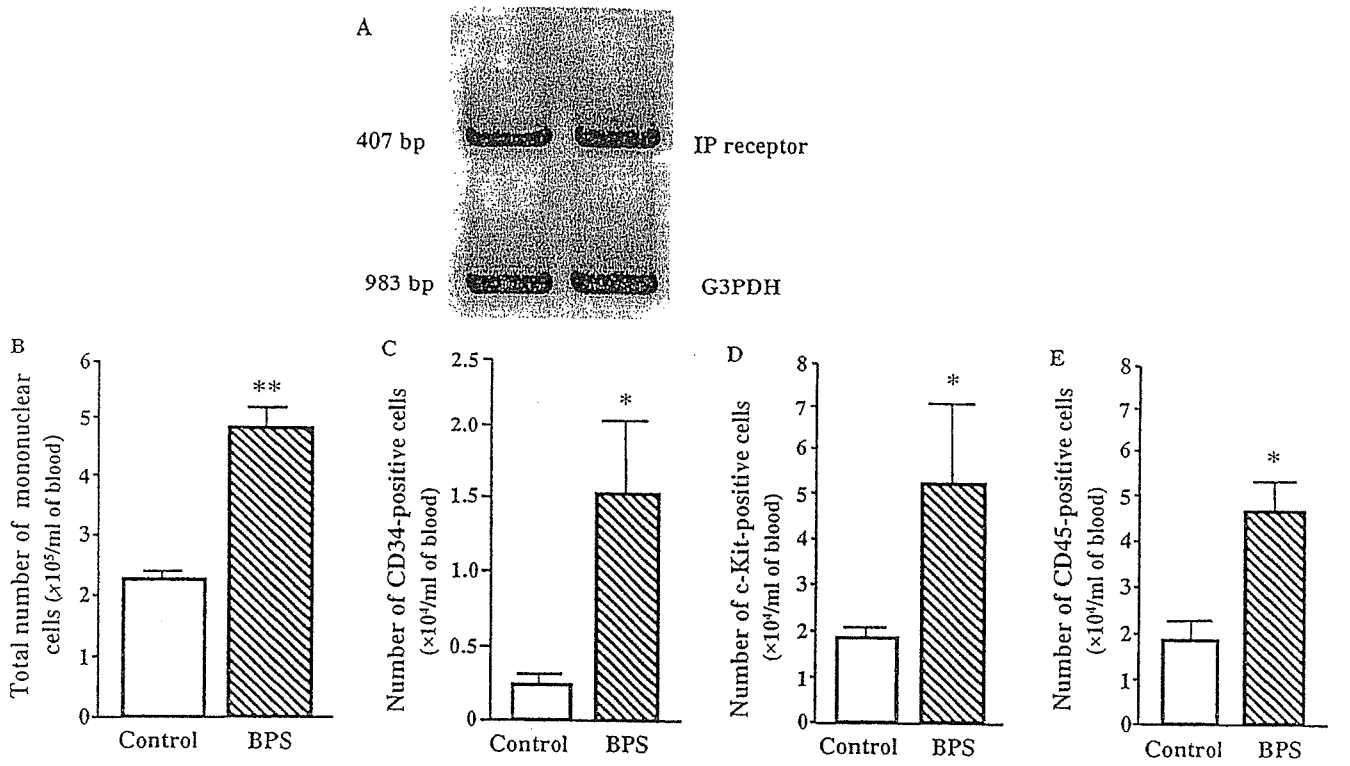

Fig. 3. BPS-induced mobilization of bone marrow cells. (A) Expression of prostacyclin receptor (IP receptor) on bone marrow cells. (B–E) Quantification of BPS-induced MNC mobilization by FACS analysis. Administration of BPS markedly increased the number of circulating progenitor cells such as CD34-positive cells and c-kit-positive cells. BPS also increased the number of CD45-positive hematopoietic lineage cells. Data are expressed as means ± SEM. $^{*}p < 0.05$, $^{**}p < 0.01$ vs. Control group.

biological activities of BPS appear to be insufficient to explain the decrease in infarct size as well as suppression of LV remodeling.

Recent studies have shown that mobilization of bone marrow cells by cytokines promotes myocardial repair and regeneration after acute myocardial infarction [5,6]. In the present study, three-day administration of BPS markedly increased the number of circulating progenitor cells such as CD34-positive cells and c-kit-positive cells in rats. In addition, treatment with BPS enhanced recruitment of bone marrow cells to the ischemic myocardium and increased capillary density in the peri-infarct area. Earlier studies have shown that CD34-positive cells have angiogenic potential to treat ischemic heart [29–31]. Also, another stem cell fraction, c-kit-positive cells have ability to repair ischemic myocardium by differentiating into vascular endothelial cells [32,33]. These findings suggest that administered BPS induces neovascularization partly via enhancement of bone marrow cell mobilization. RT-PCR demonstrated that IP receptor mRNA was expressed in bone marrow cells, indicating a direct effect of BPS on these cells. A recent study has shown that BPS increases eNOS expression in cultured endothelial cells through activation of c-AMP/Protein kinase A signal transduction [19]. Also, earlier studies have shown that eNOS plays essential role in the recruitment of EPCs to the ischemic myocardium [20]. Taken together, administered BPS may act as a potent stimulator of cell mobilization from bone marrow, although further studies are necessary to examine the underlying mechanisms.

In the present study, treatment with BPS significantly attenuated infarct size after myocardial infarction. BPS improved cardiac function and attenuated the development of LV remodeling after acute myocardial infarction, as indicated by increases in LV fractional shortening and maximum dP/dt, and decreases in LVEDP and LVDD. Taken together, BPS may attenuate myocardial infarction through enhancement of neovascularization via modification of bone marrow kinetics. Interestingly, a small fraction of mobilized bone marrow cells expressed cardiac troponin T in the ischemic myocardium in the BPS group, suggesting that BPS may partially contribute to myocardial regeneration after acute myocardial infarction. Earlier studies have demonstrated that BPS has other beneficial effects for ischemic heart disease including anti-thrombotic activity [34], inhibition of reperfusion injury [35], and prevention of coronary spasm [36], and re-stenosis [37]. These findings suggest that administration of BPS may be a promising therapy for acute myocardial infarction.

Granulocyte colony stimulating factor (G-CSF) is currently used agent for mobilization of bone marrow. Infusion of G-CSF after myocardial infarction improves LV function increasing peripheral stem cell fraction [5,38]. A recent clinical trial, however, claimed the G-CSF therapy

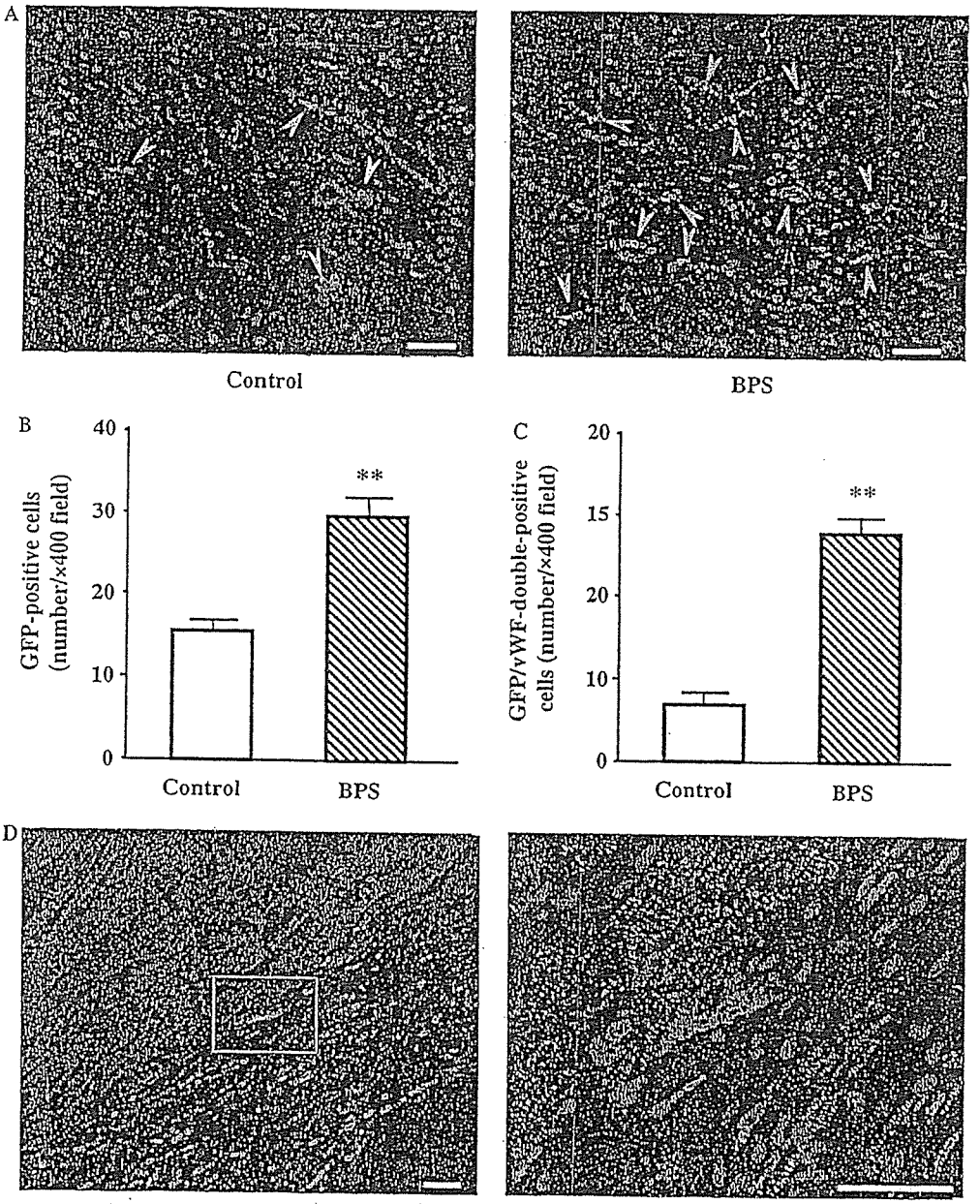

Fig. 4. BPS-induced neovascularization. (A) Representative immunofluorescent images stained with antibodies to von-Willbrand factor (vWF, red) and green fluorescent protein (GFP, green). Nuclei were counterstained with DAPI (blue). (B,C) Semi-quantitative analyses of numbers of GFP-positive cell and GFP-vWF double-positive cells in the peri-infarct area. (D) Representative immunofluorescent image of GFP-positive cells (green) expressing cardiac troponin T (red) observed in the BPS group. Scale bars = 50 μm. Data are expressed as means ± SEM. $^{**}p < 0.01$ vs. Control group.

has serious problem with re-stenosis after recanalization [39]. On the other hand, the safety of BPS has been identified in the treatment of peripheral arterial disease [12,13] and pulmonary arterial hypertension [14,15]. A randomized, controlled clinical trial failed to demonstrate therapeutic potential of prostacyclin for the treatment of severe congestive heart failure [40], which has long discouraged the pursuit of prostacyclin as a therapeutic option for the treatment of acute myocardial infarction. Interestingly, however, double-blinded, randomized, placebo-controlled, large-scale studies showed that treatment with BPS decreased vascular events in patients with peripheral arterial disease [41,42]. Thus, adequate use of BPS for early acute myocardial infarction may have beneficial effects on ischemic myocardium, although further preclinical trials are required to verify the safety and efficacy of BPS.

Conclusion

In summary, administration of BPS improved cardiac structure and function in rats with acute myocardial infarction. This beneficial effect of BPS may be mediated partly by its ability to enhance neovascularization in ischemic myocardium by mobilizing bone marrow cells.

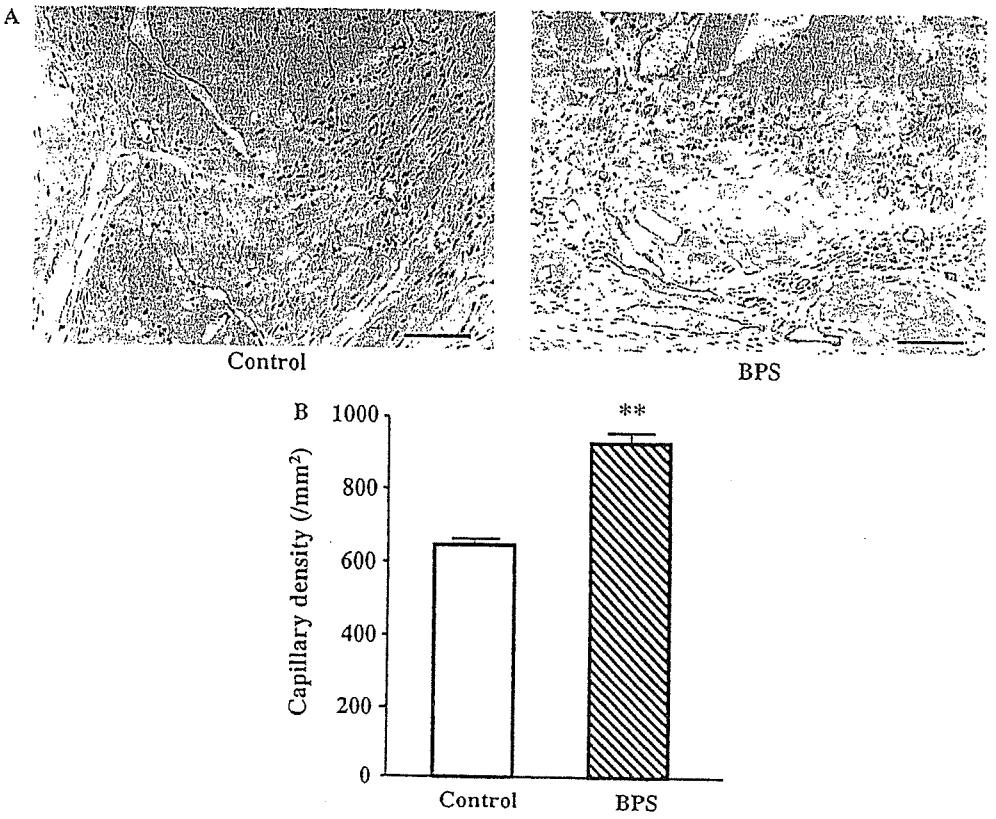

Fig. 5. (A) Representative samples stained with antibody to von Willebrand factor by bright-field DAB. (B) Quantitative analysis of capillary density in peri-infarct area. Administration of BPS increased capillary density by 37%. Scale bars = 50 μm. Data are expressed as means ± SEM. $^{**}p < 0.01$ vs. Control group.

Acknowledgment

This work was supported by research grants for Cardiovascular Disease (16C-6) from the Ministry of Health, Labor and Welfare, and for Japan Vascular Disease Research Foundation.

References

[1] A. Saraste, K. Pulkki, M. Kallajoki, K. Henriksen, M. Parvinen, L.M. Voipio-Pulkki, Apoptosis in human acute myocardial infarction, Circulation 95 (1997) 320–323.
[2] S. Shintani, T. Murohara, H. Ikeda, T. Ueno, T. Honma, A. Katoh, K. Sasaki, T. Shimada, Y. Oike, T. Imaizumi, Mobilization of endothelial progenitor cells in patients with acute myocardial infarction, Circulation 103 (2001) 2776–2779.
[3] D. Orlic, J. Kajstura, S. Chimenti, I. Jakoniuk, S.M. Anderson, B. Li, J. Pickel, R. Mckay, B. Nadal-Ginard, D.M. Bodine, A. Leri, P. Anversa, Bone marrow cells regenerate infarcted myocardium, Nature 410 (2001) 701–705.
[4] H. Oh, S.B. Bradfute, T.D. Gallardo, T. Nakamura, V. Gaussin, Y. Mishina, J. Pocius, L.H. Michael, R.R. Behringer, D.J. Garry, M.L. Entman, M.D. Schneider, Cardiac progenitor cells from adult myocardium: homing, differentiation, and fusion after infarction, Proc. Natl. Acad. Sci. USA 100 (2003) 12313–12318.
[5] D. Orlic, J. Kajstura, S. Chimenti, F. Limana, I. Jakoniuk, F. Quaini, B. Nadal-Ginard, D.M. Bodine, A. Leri, P. Anversa, Mobilized bone marrow cells repair the infarcted heart, improving function and survival, Proc. Natl. Acad. Sci. USA 98 (2001) 10344–10349.
[6] T. Asahara, T. Takahashi, H. Masuda, C. Kalka, D. Chen, H. Iwaguro, Y. Inai, M. Silver, J.M. Isner, VEGF contributes to postnatal neovascularization by mobilizing bone marrow-derived endothelial progenitor cells, EMBO J. 18 (1999) 3964–3972.
[7] T. Murata, T. Murai, T. Kanai, Y. Ogaki, K. Sanai, H. Kanda, S. Sato, N. Kajikawa, T. Umetsu, H. Matsuura, General pharmacology of beraprost sodium, Arzneimittelforschung 39 (1989) 867–876.
[8] T. Akiba, M. Miyazaki, N. Toda, Vasodilator actions of TRK-100, a new prostaglandin I2 analogue, Br. J. Pharmacol. 89 (1986) 703–711.
[9] S. Nishio, H. Matsuura, N. Kanai, Y. Fukatsu, T. Hirano, N. Nishikawa, K. Kameoka, T. Umetsu, The in vitro and ex vivo antiplatelet effect of TRK-100, a stable prostacyclin analog, in several species, Jpn J. Pharmacol. 47 (1988) 1–10.
[10] J.L. Demolis, A. Robert, M. Mouren, C. Funck-Brentano, P. Jaillon, Pharmacokinetics and platelet antiaggregating effects of beraprost, an oral stable prostacyclin analogue, in healthy volunteers, J. Cardiovasc. Pharmacol. 22 (1993) 711–716.
[11] P. Nony, P. Ffrench, P. Girard, S. Delair, S. Azoulay, J.P. Girre, M. Dechavanne, J.P. Boissel, Platelet-aggregation inhibition and hemodynamic effects of beraprost sodium, a new oral prostacyclin derivative: a study in healthy male subjects, Can. J. Physiol. Pharmacol. 74 (1996) 887–893.
[12] M. Murakami, M. Watanabe, H. Furukawa, H. Nakahara, The prostacyclin analogue beraprost sodium prevents occlusion of bypass grafts in patients with lower extremity arterial occlusive disease: a 20-year retrospective study, Ann. Vasc. Surg. 19 (2005) 838–842.
[13] L.T. Cooper, Beraprost for the treatment of intermittent claudication, J. Am. Coll. Cardiol. 41 (2003) 1679–1686.
[14] Y. Okano, T. Yoshioka, A. Shimouchi, T. Satoh, T. Kunieda, Orally active prostacyclin analogue in primary pulmonary hypertension, Lancet 349 (1997) 1365.

[15] N. Nagaya, M. Uematsu, Y. Okano, T. Satoh, S. Kyotani, F. Sakamaki, N. Nakanishi, K. Miyatake, T. Kunieda, Effect of orally active prostacyclin analogue on survival of outpatients with primary pulmonary hypertension, J. Am. Coll. Cardiol. 34 (1999) 1188–1192.
[16] A.M. Lefer, M.L. Ogletree, J.B. Smith, M.J. Silver, K.C. Nicolaou, [illegible] G P. Gasic, Prostacyclin: a potentially valuable agent [illegible] acute myocardial ischemia, Science 200 (1978) 52–54.
[17] B.I. Jugdutt, G.M. Hutchins, B.H. Bulkley, L.C. Becker, Dissimilar effects of prostacyclin, prostaglandin E1, and prostaglandin E2 on myocardial infarct size after coronary occlusion in conscious dogs, Circ. Res. 49 (1981) 685–700.
[18] J.A. Melin, L.C. Becker, Salvage of ischemic myocardium by prostacyclin during experimental myocardial infarction, J. Am. Coll. Cardiol. 2 (1983) 279–286.
[19] K. Niwano, M. Arai, K. Tomaru, T. Uchiyama, Y. Ohyama, M. Kurabayashi, Transcriptional stimulation of the eNOS gene by the stable prostacyclin analogue beraprost is mediated through cAMP-responsive element in vascular endothelial cells: close link between PGI2 signal and NO pathways, Circ. Res. 93 (2003) 523–530.
[20] A. Aicher, C. Heeschen, C. Mildner-Rihm, C. Urbich, C. Ihling, K. Technau-Ihling, A.M. Zeiher, S. Dimmeler, Essential role of endothelial nitric oxide synthase for mobilization of stem and progenitor cells, Nat. Med. 9 (2003) 1370–1376.
[21] T. Nishikimi, K. Uchino, E.D. Frohlich, Effects of α1-adrenergic blockade on intrarenal hemodynamics in heart failure rats, Am. J. Physiol. Regul. Integr. Comp. Physiol. 262 (1998) R198–R203.
[22] P.S. Douglas, N. Reichek, T. Plappert, A. Muhammad, M.G. St John Sutton, Comparison of echocardiographic methods for assessment of left ventricular shortening and wall stress, J. Am. Coll. Cardiol. 9 (1987) 945–951.
[23] Y.W. Chien, R.W. Barbee, A.A. Macphee, E.D. Frohlich, N.C. Trippondo, Increased ANF secretion after volume expansion is preserved in rats with heart failure, Am. J. Physiol. 254 (1988) R185–R191.
[24] T. Ito, A. Suzuki, E. Imai, M. Okabe, M. Hori, Bone marrow is a reservoir of repopulating mesangial cells during glomerular remodeling, J. Am. Soc. Nephrol. 12 (2001) 2625–2635.
[25] P.J. Simpson, R.F. Todd 3rd, J.C. Fantone, J.K. Mickelson, J.D. Griffin, B.R. Lucchesi, Reduction of experimental canine myocardial reperfusion injury by a monoclonal antibody (anti-Mo1, anti-CD11b) that inhibits leukocyte adhesion, J. Clin. Invest. 81 (1988) 624–629.
[26] W.W. Nichols, J. Mehta, T.J. Wargovich, D. Franzini, D. Lawson, Reduced myocardial neutrophil accumulation and infarct size following thromboxane synthetase inhibitor or receptor antagonist, Angiology 40 (1989) 209–221.
[27] M. Kainoh, R. Imai, T. Nakadake, M. Hattori, S. Nishio, Prostacyclin and beraprost sodium as suppressors of activated rat polymorphonuclear leukocytes, Biochem. Pharmacol. 39 (1990) 477–483.
[28] Y. Ueno, Y. Miyauchi, S. Nishio, Beraprost sodium protects occlusion/reperfusion injury in the dog by inhibition of neutrophil migration, Gen. Pharmacol. 25 (1994) 427–432.
[29] A. Kawamoto, T. Tkebuchava, J. Yamaguchi, H. Nishimura, Y.S. Yoon, C. Milliken, S. Uchida, O. Masuo, H. Iwaguro, H. Ma, A. Hanley, M. Silver, M. learney, D.W. Losordo, J.M. Isner, T. Asahara, Intramyocardial transplantation of autologous endothelial progenitor cells for therapeutic neovascularization of myocardial ischemia, Circulation 107 (2003) 461–468.
[30] A. Kawamoto, T. Asahara, D.W. Losordo, Transplantation of endothelial progenitor cells for therapeutic neovascularization, Cardiovasc. Radiat. Med. 3 (2002) 221–225.
[31] A. Weber, I. Pedrosa, A. Kawamoto, N. Himes, J. Munasinghe, T. Asahara, N.M. Rofsky, D.W. Losordo, Magnetic resonance mapping of transplanted endothelial progenitor cells for therapeutic neovascularization in ischemic heart disease, Eur. J. Cardiothorac. Surg. 26 (2004) 137–143.
[32] J. Kajstura, M. Rota, B. Whang, S. Cascapera, T. Hosoda, C. Bearzi, D. Nurzynska, H. Kasahara, E. Zias, M. Bonafe, B. Nadal-Ginard, D. Torella, A. Nascimbene, F. Quaini, K. Urbanek, A. Leri, P. Anversa, Bone marrow cells differentiate in cardiac cell lineages after infarction independently of cell fusion, Circ. Res. 96 (2005) 127–137.
[33] R. Lanza, M.A. Moore, T. Wakayama, A.C. Perry, J.H. Shieh, J. Hendrikx, A. Leri, S. Chimenti, A. Monsen, D. Nurzynska, M.D. West, J. Kajstura, P. Anversa, Regeneration of the infarcted heart with stem cells derived by nuclear transplantation, Circ. Res. 94 (2004) 820–827.
[34] Y. Uchida, T. Hanai, K. Hasegawa, K. Kawamura, T. Oshima, Recanalization of obstructed coronary artery by intracoronary administration of prostacyclin in patients with acute myocardial infarction, Adv. Prostaglandin Thromboxane Leukot. Res. 11 (1983) 377–383.
[35] C.Y. Xiao, A. Hara, Yuhki K, T. Fujino, H. Ma, Y. Okada, O. Takahata, T. Yamada, T. Murata, S. Narumiya, F. Ushikubi, Roles of prostaglandin I(2) and thromboxane A(2) in cardiac ischemia–reperfusion injury: a study using mice lacking their respective receptors, Circulation 104 (2001) 2210–2215.
[36] A. Szczeklik, J. Szczeklik, R. Nizankowski, P. Gluszko, Prostacyclin for unstable angina, N. Engl. J. Med. 303 (1980) 881.
[37] M.L. Knudtson, V.F. Flintoft, D.L. Roth, J.L. Hansen, H.J. Duff, Effect of short-term prostacyclin administration on restenosis after percutaneous transluminal coronary angioplasty, J. Am. Coll. Cardiol. 15 (1990) 691–697.
[38] F. Kuethe, H.R. Figulla, M. Herzau, M. Voth, M. Fritzenwanger, T. Opfermann, K. Pachmann, A. Krack, H.G. Sayer, D. Gottschild, G.S. Werner, Treatment with granulocyte colony-stimulating factor for mobilization of bone marrow cells in patients with acute myocardial infarction, Am. Heart J. 150 (2005) 115.
[39] H.J. Kang, H.S. Kim, S.Y. Zhang, K.W. Park, H.J. Cho, B.K. Koo, Y.J. Kim, D. Soo Lee, D.W. Sohn, K.S. Han, B.H. Oh, M.M. Lee, Y.B. Park, Effects of intracoronary infusion of peripheral blood stem-cells mobilised with granulocyte-colony stimulating factor on left ventricular systolic function and restenosis after coronary stenting in myocardial infarction: the MAGIC cell randomised clinical trial, Lancet 363 (2004) 751–756.
[40] R.M. Califf, K.F. Adams, W.J. McKenna, M. Gheorghiade, B.F. Uretsky, S.E. McNulty, H. Darius, K. Schulman, F. Zannad, E. Handberg-Thurmond, F.E. Harrell Jr., W. Wheeler, J. Soler-Soler, K. Swedberg, A randomized controlled trial of epoprostenol therapy for severe congestive heart failure: The Flolan International Randomized Survival Trial (FIRST), Am. Heart J. 134 (1997) 44–54.
[41] M. Lievre, S. Morand, B. Besse, J.N. Fiessinger, J.P. Boissel, Oral beraprost sodium, a prostaglandin I(2) analogue, for intermittent claudication: a double-blind, randomized, multicenter controlled trial. Beraprost et Claudication Intermittente (BERCI) Research Group, Circulation 102 (2000) 426–431.
[42] E.R. Mohler 3rd, W.R. Hiatt, J.W. Olin, M. Wade, R. Jeffs, A.T. Hirsch, Treatment of intermittent claudication with beraprost sodium, an orally active prostaglandin I2 analogue: a double-blinded, randomized, controlled trial, J. Am. Coll. Cardiol. 41 (2003) 1679–1686.

Unblinded Pilot Study of Autologous Transplantation of Bone Marrow Mononuclear Cells in Patients With Thromboangiitis Obliterans

Koji Miyamoto, MD; Kazuhiro Nishigami, MD; Noritoshi Nagaya, MD; Koichi Akutsu, MD; Masaaki Chiku, MD; Masataka Kamei, MD; Toshihiro Soma, MD; Shigeki Miyata, MD; Masahiro Higashi, MD; Ryoichi Tanaka, MD; Takeshi Nakatani, MD; Hiroshi Nonogi, MD; Satoshi Takeshita, MD

Background—The short-term clinical benefits of bone marrow mononuclear cell transplantation have been shown in patients with critical limb ischemia. The purpose of this study was to assess the long-term safety and efficacy of bone marrow mononuclear cell transplantation in patients with thromboangiitis obliterans.

Methods and Results—Eleven limbs (3 with rest pain and 8 with an ischemic ulcer) of 8 patients were treated by bone marrow mononuclear cell transplantation. The patients were followed up for clinical events for a mean of 684±549 days (range 103 to 1466 days). At 4 weeks, improvement in pain was observed in all 11 limbs, with complete relief in 4 (36%). Pain scale (visual analog scale) score decreased from 5.1±0.7 to 1.5±1.3. An improvement in skin ulcers was observed in all 8 limbs with an ischemic ulcer, with complete healing in 7 (88%). During the follow-up, however, clinical events occurred in 4 of the 8 patients. The first patient suffered sudden death at 20 months after transplantation at 30 years of age. The second patient with an incomplete healing of a skin ulcer showed worsening of the lesion at 4 months. The third patient showed worsening of rest pain at 8 months. The last patient developed an arteriovenous shunt in the foot at 7 months, which spontaneously regressed by 1 year.

Conclusions—In the present unblinded and uncontrolled pilot study, long-term adverse events, including death and unfavorable angiogenesis, were observed in half of the patients receiving bone marrow mononuclear cell transplantation. Given the current incomplete knowledge of the safety and efficacy of this strategy, careful long-term monitoring is required for future patients receiving this treatment. (*Circulation.* **2006;114:2679-2684.**)

Key Words: angiogenesis ■ collateral circulation ■ endothelium ■ peripheral vascular diseases

The clinical consequences of severe peripheral arterial disease or critical limb ischemia include rest pain and the loss of tissue integrity in the distal limb.[1–3] Therapeutic options for such patients are limited. These conditions are often refractory to conservative measures and are typically unresponsive to drug therapy. When vascular obstruction involves a long segment or is widespread, percutaneous revascularization may not be feasible. Surgical therapy, consisting of arterial bypass or amputation, is complicated by variable morbidity and mortality, and its effectiveness depends on the short- and long-term patencies of the conduit employed. Therapeutic angiogenesis thus constitutes a potential alternative treatment strategy for such patients.[4,5]

Previous investigators have suggested that endothelial progenitor cells, originating from bone marrow, circulate in adult peripheral blood and participate in postnatal neovascularization.[6–8] Subsequent experiments have shown that bone marrow or bone marrow–derived cells have the potential to stimulate angiogenesis and thereby modulate the hemodynamic deficit in ischemic limbs in vivo.[9,10] The Therapeutic Angiogenesis by Cell Transplantation (TACT) study first demonstrated that the magnitude of angiogenesis stimulated by these cells is sufficient to constitute a therapeutic benefit in patients with critical limb ischemia.[11] In that study, the investigators injected bone marrow mononuclear cells (BM-MNCs) into the ischemic limb of patients and documented a significant improvement in the hemodynamic deficit as well as the relief of ischemic symptoms. Although the TACT

Editorial p 2581
Clinical Perspective p 2684

Received June 9, 2006; revision received September 19, 2006; accepted September 21, 2006.

From the Departments of Medicine (K.M., K.N., K.A., M.C., H.N., S.T.), Regenerative Medicine and Tissue Engineering (N.N.), Anesthesiology (M.K.), Transfusion Medicine (S.M.), Radiology (M.H., R.T.), and Organ Transplantation (T.N.), National Cardiovascular Center, Osaka; and the Department of Clinical Laboratory (T.S.), Osaka Minami Medical Center, Osaka, Japan.

Correspondence to Dr Satoshi Takeshita, MD, FACC, Department of Medicine (Cardiology), National Cardiovascular Center, 5-7-1 Fujishiro-dai, Suita, Osaka 565-8565, Japan. E-mail stake@muse.ocn.ne.jp

Circulation is available at http://www.circulationaha.org

DOI: 10.1161/CIRCULATIONAHA.106.644203